

AN ABSTRACT OF THE THESIS OF

Saangrut Sangplung for the degree of Master of Science in Mechanical Engineering presented on August 29, 2003. Title: Solutions of Plate Equation for the Prediction of Ink Droplets in Inkjet Cartridges.

Abstract approved: _____

Mark F. Costello

Droplet formation in inkjet cartridges has been studied for several decades to improve print qualities. Currents and rigid nozzle plates are used inside the cartridge to fix the size of droplets exiting the chamber. This research is focused on studying the effect of nozzle flexibility on droplet formation. A flexible nozzle can be modeled as an flexible annular plate with a clamped outside edge.

In this thesis, plate vibration equations are studied for an annular shape. An analytical solution is formed for the small deflection plate equation. To solve the large deflection plate vibration equation, Galerkin's method is used. Droplet formation is predicted by a one dimensional fluid dynamic model. An integrated plate vibration and droplet formation model is created with these basic building blocks. Results from simulation indicate flexible plates yield shorter droplet breakoff time and longer breakoff distance while generating a slightly droplet compared to a rigid nozzle.

© Copyright by Saangrut Sangplung

August 29, 2003

All Righted Reserved

**SOLUTIONS OF PLATE EQUATION FOR
THE PREDICTION OF INK DROPLETS IN INKJET CARTRIDGES**

By

Saangrut Sangplung

A THESIS

Submitted to

Oregon State University

**In partial fulfillment of
The requirements for the
degree of
Master of Science**

Presented August 29, 2003

Commencement June 2004

Master of Science thesis of Saangrut Sangplung presented on August 29 2003.

APPROVED:



Major Professor, representing Mechanical Engineering



Head of Department of Mechanical Engineering



Dean of the Graduate School

I understand that my thesis will become part of the permanent collection of Oregon State University libraries. My signature below authorizes release of my thesis to any reader upon request.



Saangrut Sangplung, Author

ACKNOWLEDGEMENT

I would like to express my sincere gratitude to Dr. Mark F. Costello for his guidance and support during my graduate study. I would also like to thank my graduate committee members for guidance during my studies.

I would also like to thank sincerely my parents, Mr. Nakorn and Mrs Jarasorn Sangplung, as well as my sister, Wassama, for their encouragement and support during study.

TABLE OF CONTENTS

	<u>Page</u>
1. INTRODUCTION.....	1
2. LITERATURE REVIEW.....	3
2.1 Plate Vibration Equation.....	3
2.2 Solutions of Plate Vibration Equation.....	3
2.3 Galerkin's Method.....	5
2.4 Droplet Formation.....	6
3. MATHEMATICAL MODEL.....	7
3.1 Coordinate System.....	7
3.2 Small Deflection Plate Dynamic Equation of Motion.....	8
3.3 Plate Equation in Polar Coordinate.....	10
3.4 Axis Symmetrical Stress Distribution.....	13
3.5 Damping Coefficient of Plate.....	14
3.6 Plate Equation under Combined Lateral and In-Plane Loads.....	14
3.7 Droplet Formation Model.....	19
4. SOLUTIONS OF PLATE EQUATION.....	21
4.1 Analytical Solutions of Clamped Annular Plate.....	23
4.1.1 Free Vibration Solutions of Clamped Annular Plate.....	23
4.1.2 Forced Vibration Solutions of Clamped Annular Plate.....	27
4.2 Numerical Solutions of Large Deflection Equation.....	29
5. RESULTS.....	34
5.1 Surface Deflection of Small Deflection Plate Equation.....	34
5.2 Surface Deflection of Large Deflection Plate Equation.....	35
5.3 Droplet Formation Simulation.....	38
6. CONCLUSION.....	50
6.1 Conclusion.....	50
6.2 Recommendations for the Future Research.....	52

LIST OF FIGURES

<u>Figure</u>	<u>Page</u>
3.1 Plate element in polar coordinate.....	7
3.2 Free body diagram of dynamic system of plate element.....	8
3.3 Free body diagram of plate element in polar coordinate.....	11
3.4 Force on the midplane of plate element.....	14
3.5 Geometry of the liquid column from orifice.....	19
4.1 Annular clamped plate.....	21
5.1 Comparison of damped and undamped solutions of inner node's deflection of annular plate.....	35
5.2 Comparison of maximum deflection between Energy method and Galerkin method.....	36
5.3a Comparison between small and large deflection at 1 Pa force amplitude.....	37
5.3b Comparison between small and large deflection at 5 KPa force amplitude.....	38
5.4 Experimental model of plate vibration.....	39
5.5 Pulse input excitation.....	40
5.6a Liquid column shape at $t= 0.0000822$ s.....	41
5.6b Liquid column shape at $t= 0.00016029$ s.....	42
5.6c Liquid column shape at $t= 0.0001619$ s.....	43
5.7 Relation between pressure and breakoff time.....	44
5.8 Relation between pressure and radius of droplet after breakoff.....	45
5.9 Pressure vs distance of droplet after breakoff.....	46
5.10 Young modulus vs breakoff time.....	47
5.11 Young modulus vs droplet size.....	48
5.12 Young modulus vs breakoff distance.....	49

LIST OF TABLES

<u>Table</u>	<u>Page</u>
4.1 The eigenfrequencies of $[A_f]$	26
6.1 Characteristic of droplet formation with high flexibility and rigidity.....	51

NOMENCLATURE

- $[A_f]$ = Constant matrix for boundary conditions of annular plate
- A = Area
- A_i, B_i, C_i, E_i, F_i = Constant of mode i
- A_n, B_n = Constant
- a, b = Outer and inner radii of plate
- c = Damping coefficient
- c_1, c_2, c_3, c_4 = Mode shape parameters
- c_5, c_6, c_7, c_8 = Mode shape parameters
- D = Flexural rigidity
- E = Modulus of elasticity
- ϵ = Error constant
- F_0 = Force amplitude per unit area
- G = Modulus of elasticity in shear
- H_{ci} = Modal constant
- h = Thickness
- I_n, K_n = Modified Bessel function of order n
- \bar{I}, \bar{J} = Unit vectors in X-Y planes
- i, N, n = Integers, numerical factor
- J_n, Y_n = Bessel function of order n
- M_x, M_y = Bending moments per unit distance on X and Y planes
- M_{xy} = Twisting moment per unit distance on X plane
- M_r, M_θ = Radial and tangential moments per unit distance
- $M_{r\theta}$ = Twisting moment per unit distance on radial plane
- N_x, N_y = Bending tensile forces per unit distance on X and Y planes
- N_{xy} = Twisting tensile force per unit distance on X plane
- Q_x, Q_y = Shear force per unit distance on X and Y planes

- Q_r, Q_θ = Radial and tangential shear forces per unit distance
 P = Distributed force
 r, θ = Distance polar coordinate
 t = Time
 u, v, w = Displacements in x, y and z directions
 \tilde{w} = Approximate Displacements in z directions
 x, y, z = Distance rectangular coordinate
 η = Error correction constant
 β = Eigenfrequency
 $\varepsilon_x, \varepsilon_y, \varepsilon_z$ = Normal strains in X, Y and Z directions
 $\gamma_{xy}, \gamma_{yz}, \gamma_{zx}$ = Shear strains in XY, YZ and ZX planes
 ρ = Density
 ω_n = Natural frequency
 ω_d = Damping natural frequency
 ν = Poisson's ratio
 ζ_n = Damping ratio
 δ_{ij} = Constant of mode i and j
 Ω_i = Orthogonalized constant of mode i
 ϕ = Airy stress function
 μ, ψ = Constant of interval integration result of Othogonalization

SOLUTIONS OF PLATE EQUATION FOR THE PREDICTION OF INK DROPLETS IN INKJET CARTRIDGES

CHAPTER 1 **INTRODUCTION**

The inkjet printer is one of the most popular types of printers at present. One of the significant parts in this type of printer is the cartridge, which determines the efficiency and quality of printing. The main purpose of the cartridge is to generate ink droplets and transfer them onto the printing area. The size of the microdroplet is fixed by the size of the hole at the nozzle plate. Normally, a microdroplet is generated by creating high pressure in the ink chamber to break surface tension and viscous force. There are many methods to generate a droplet, but most of these methods are based on the principle of a pressure difference to eject a droplet from the nozzle. This process is called “actuation.” Actuation is a basic concept of creating a pressure difference between the inside and outside of the nozzle.

This thesis emphasizes the effect of nozzle plate flexibility to an droplet formation. The flexibility behavior of a nozzle plate is studied to determine its relation to surface deflection and velocity. In turn, the surface velocity is significant to the droplet formation for a moving nozzle. In the process of research, thin plate theory is applied to an annular plate model to find surface deflection and velocity. Then, the thin plate equation is integrated with a one dimensional droplet formation equation to predict the formation of a droplet.

This research can be divided into two work elements: nozzle plate vibration and droplet formation for moving nozzle plates. These two models are integrated together to predict droplet formation. As mentioned before, the study of flexible nozzle plate vibration is performed in this research research under the guidance of Dr Costello of the Mechanical Engineering

Department, Oregon State University. On the other hand, the research of droplet formation is conducted by Mr. Yang, a fellow graduate student in this project group, under the guidance of Dr. Liburdy of the Mechanical Engineering Department, Oregon State University.

The thesis is organized as follows. Chapter 2 presents a literature review for pertinent topics. The development of the large deflection plate vibration equations, the mathematical model of a nozzle plate, and the model of droplet formation are described in Chapter 3. Chapter 4 demonstrates the use of analytical and numerical approaches to solve linear and nonlinear equation appropriately. The simulation results of plate vibration and droplet formation are presented in Chapter 5. Chapter 6 consists of research conclusions and recommendations for future research.

CHAPTER 2

LITERATURE REVIEW

At the beginning of this research, the fundamental approaches and previous solutions are reviewed as a resource and reference for solving the problem in this project. The project can be divided into three categories; plate vibration equations and their solutions, numerical methods, and droplet formation.

2.1 Plate Vibration Equation

The study of plate vibration has its origin with the experimental work of Chladni [6] in the early nineteenth century who demonstrated the nodal patterns of a square plate in lateral bending. The theoretical background of the theory of plates was laid by Germain and Lagrange around 1816. However, there was considerable discussion on boundary conditions produced in this work and it was left to Kirchoff and Kelvin around 1850 to settle this matter. Since then a great many cases of plate-bending problem have been solved analytically by Navier (1864), Kirchoff (1882), Von Karman (1910) and Levy (1942), and numerically by Galkerin (1930), Wahl (1963), and others.

There are also a few books on thin plate theory. The classical text on *The Theory of Plates and Shells* by S.P. Timochenko (1959) is still a good reference book, even though it is written nearly more than five decades ago.

2.2 Solutions of Plate Equation

The solutions of plate equation can be determined by both analytical method and numerical method. The monograph *Vibration of Plates*, 1969, written by Professor A.W. Leissa and published by NASA is useful for finding analytical solutions of plate equations. Many other analytical treatments exist, including solutions for a 2-D plate (Turcotte and Schubert, 1982), for the point-load response of a semi-infinite plate (Wessel, 1996), and a more complete treatment of the axisymmetric case (Lambeck

and Makiboglu, 1980), as well as for stress-dependent flexural rigidity (Wessel, 1993). Southwell (1922) derived equations for annular plate clamped around the inner boundary and free at the outside edge. Vogel and Skinner (1965) studied nine combinations of boundary conditions: simply supported, clamped and free edges at the inner and outer boundaries. Data references are also available from Leissa (1969).

Annular and perforated plates are often in contact with a fluid on one or both sides. It is well known that natural frequencies of a thin-walled structure are strongly affected by the presence of a heavy fluid. Therefore, the study of annular plates in contact with a fluid has practical interest. Works in the literature on this topic include De Santo (1981), Kubota and Suzuki (1984), Amabili and Frosali (1994) and Amabili (1994). The contribution from De Santo (1981) is an experimental investigation of perforated plates used in nuclear reactors. In the work of Kubota and Suzuki (1984), annular plates vibrating in an annular cylindrical cavity filled with a fluid were theoretically and experimentally studied. In the paper by Amabili and Frosali (1994), free vibrations of annular plates placed on a free surface were theoretically investigated. Experimental coefficients useful to compute natural frequencies of annular plates placed on a free fluid surface or completely immersed in water were given in the work of Amabili (1994).

In the design of thin plates that bend under lateral and edge loading, formulas based on the Kirchoff's theory, which neglects stretching and shearing in middle surface, are quite satisfactory in providing small deflection comparing to the thickness. In the case where deflection is equal or greater than the plate, Kirchoff's theory yields results that are considerably in error. Then, Von Karman theory is employed. Von Karman's equation is a nonlinear equation, which can be solved by approximate solutions. A number of approximate solutions have been developed for the cases of rectangular and circular plates that reported S. Levy (1942), Wah T (1963), Srinivasan (1965) and etc.

2.3 Galerkin Method

A common step in many structural, acoustic and fluid applications involves the solution of a partial differential equation (PDE) modeling the physics of a system. Due to the complexity of many problems, however, analytic solutions usually cannot be obtained and one must numerically approximate the governing equations. From separation of variables and truncation of the resulting infinite series, approximations in the form of modal expansions involving Bessel components can occasionally be used to approximate PDE dynamics. In the category of spectral methods for circular geometries, Galerkin, collocation and tau methods have been studied with the choice of method depending upon the problem being considered.

To date, much of this research has centered around the simulation of fluid flow and boundary layer growth and in these cases, emphasis has usually been placed on collocation due its success in handling complex boundary conditions, variable coefficients, and strong nonlinearities (Orszag (1983) and Patera (1981)). Galerkin methods for flows on spheres are discussed by Orszag (1974), but this is done primarily in the context of Fourier expansions involving the strong form of the modeling flow equations with only a brief discussion concerning Legendre bases being included. This reference also includes a general comparison between the results obtained with surface harmonics (eigenfunctions of the Laplacian), modified Robert functions and Fourier series using collocation and Galerkin methods in the presence of the coordinate singularity. The use of the modified Robert functions and techniques for improving their conditioning and employing fast transforms is further addressed by Bouaoudia (1991).

The paper of Bank and Smith (1993) presents a Galerkin method for linear or weakly nonlinear problems having circular or cylindrical domains using piecewise spline and spectral bases. Two areas from which they draw examples are structural dynamics and acoustics.

2.4 Droplet Formation

The phenomenon of droplet formation in a liquid jet has been studied by many authors. The earliest analysis appears to be that of Rayleigh, who made a linearized stability analysis of a nonviscous liquid jet. Later on, both linear and nonlinear studies have been performed. Linearization makes closed-form solutions possible including solutions for stability of the stream and for drop breakup time under a given initial perturbation and external excitation. Such closed-form solutions have been described by Sweet (1965) and Kamphoefner (1972). Also, for one-dimensional numerical Model of droplet, Adams and Roy (1986) present a Macormack predictor-corrector algorithm to solve one-dimensional model equations of drop development from a drop-on-demand ink jet.

CHAPTER 3

MATHEMATICAL MODEL

This chapter emphasizes the mathematical models which consist of small deflection and large deflection plate equations. To better understand each model, this chapter also explains in depth the process involving the development of both linear and nonlinear models. The topics are listed as follow: Coordinate System, Plate Dynamic Equation of Motion, Plate Equation in Polar Coordinate, Axis Symmetrical Stress Distribution, Damping Coefficient of Plate, Plate Equation under the Combined Lateral and In-Plane Loads, and Droplet Formation Model.

3.1 Coordinate System

The derivation of classical plate equations is based on Cartesian coordinates (x, y, z) . Plate dimensions are defined in X-Y plane called the midplane. Transverse deflection of each element is in Z-axis, perpendicular to the midplane. The thin plate equation in Cartesian coordinate is converted to polar coordinates (r, θ, z) for circular geometry. The polar coordinate set (r, θ) and the rectangular set (x, y) and related by equation (3.1).

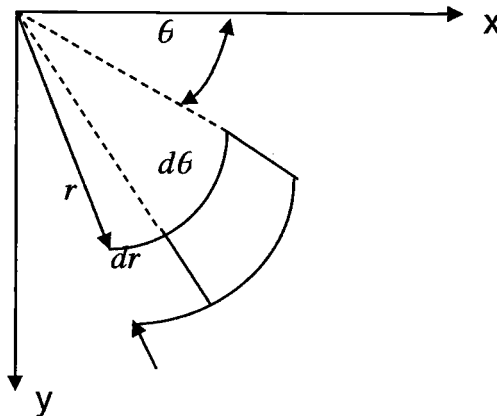


Figure 3.1 Plate element in polar coordinate

$$\left. \begin{aligned} x &= r \cdot \cos(\theta) & y &= r \cdot \sin(\theta) \\ r^2 &= x^2 + y^2 & \theta &= \tan^{-1}\left(\frac{y}{x}\right) \end{aligned} \right\} \quad (3.1)$$

3.2 Small Deflection Plate Dynamic Equation of Motion

In order to develop the equation of motion for a vibration disk, classical plate theory is employed. The stress resultant produces bending and twisting moments in terms of the curvatures and deflection.

In derivation of the dynamic equation of motion for a thin plate, the force and acceleration method is employed. For the equilibrium of dynamic system, the free body diagram on an element subjected to a vertical pressure is shown in Figure 3.2, neglecting gravity force.

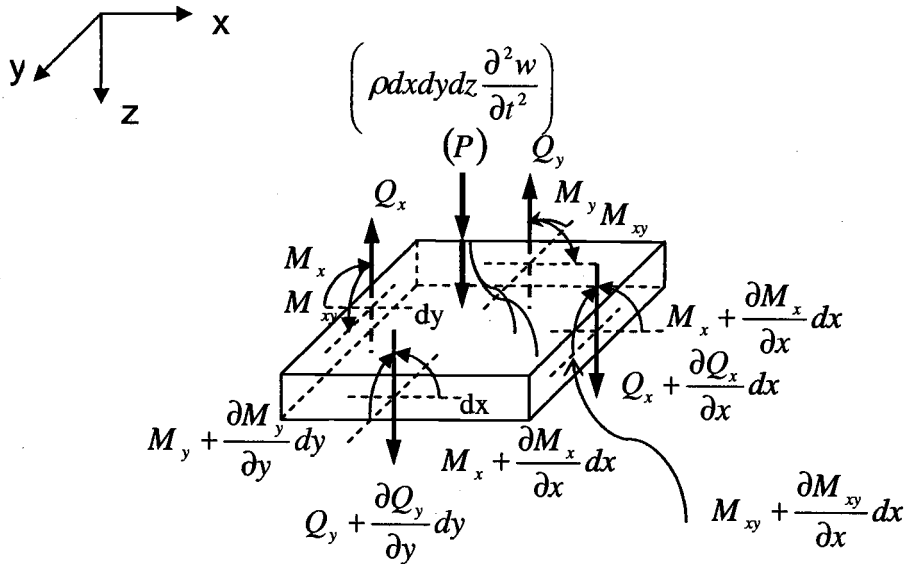


Figure 3.2 Free body diagram of dynamic system of plate element

The sum of forces in vertical direction leads to equation (3.2).

$$\frac{\partial Q_x}{\partial x} + \frac{\partial Q_y}{\partial y} + P = \rho h \frac{\partial^2 w}{\partial t^2} \quad (3.2)$$

where P is the distribute load applied to the whole membrane and the moment equilibrium about the mass center is shown as equations (3.3).

$$\frac{\partial M_{xy}}{\partial x} + \frac{\partial M_y}{\partial y} + Q_y = 0 \quad (3.3a)$$

$$\frac{\partial M_{xy}}{\partial y} + \frac{\partial M_x}{\partial x} - Q_x = 0 \quad (3.3b)$$

The expressions of vertical shear forces, Q_x and Q_y , can be expressed in terms of deflection, w , by substituting equations of moment components of cut plane edge into equation (3.3). Then, the simplified expressions are shown in equation (3.4).

$$Q_x = -D \frac{\partial}{\partial x} \left(\frac{\partial^2 w}{\partial x^2} + \frac{\partial^2 w}{\partial y^2} \right) = -D \frac{\partial}{\partial x} (\nabla^2 w) \quad (3.4a)$$

$$Q_y = -D \frac{\partial}{\partial y} \left(\frac{\partial^2 w}{\partial x^2} + \frac{\partial^2 w}{\partial y^2} \right) = -D \frac{\partial}{\partial y} (\nabla^2 w) \quad (3.4b)$$

Manipulation of equation (3.3) for shear forces leads to plate dynamic equation of motion as shown in equation (3.5).

$$-D \left(\frac{\partial^4 w}{\partial x^4} + 2 \frac{\partial^4 w}{\partial x^2 \partial y^2} + \frac{\partial^4 w}{\partial y^4} \right) + P = \rho h \frac{\partial^2 w}{\partial t^2} \quad (3.5)$$

where $D = \frac{-E \cdot h^3}{12(1-\nu^2)}$

Introducing the Laplacian operator, equation (3.5) can be shown in concise form as in equation (3.6).

$$-D(\nabla^4 w) + P = \rho h \frac{\partial^2 w}{\partial t^2} \quad (3.6)$$

and $\nabla^2 = \frac{\partial^2}{\partial x^2} + \frac{\partial^2}{\partial y^2}$ (3.7)

$$\nabla^4 = (\nabla^2)^2 = \frac{\partial^4}{\partial x^4} + 2 \frac{\partial^4}{\partial x^2 \partial y^2} + \frac{\partial^4}{\partial y^4} \quad (3.8)$$

3.3 Plate Equation in Polar Coordinates

The classical plate equation of motion in rectangular coordinates can be transformed into polar coordinate by using equation (3.1) accompanied with the chain-rule derivative formula. Referring to figure 3.1 together with equation (3.1)

$$\left. \begin{aligned} \frac{\partial r}{\partial x} &= \frac{r}{x} = \cos(\theta) & \frac{\partial r}{\partial y} &= \frac{r}{y} = \sin(\theta) \\ \frac{\partial \theta}{\partial x} &= -\frac{\sin(\theta)}{r} & \frac{\partial \theta}{\partial y} &= \frac{\cos(\theta)}{r} \end{aligned} \right\} \quad (3.9)$$

To find the deflection as a function of r and θ , the chain rule associated with equation (3.9) leads to equation (3.10).

$$\begin{aligned} \frac{\partial w}{\partial x} &= \frac{\partial w}{\partial r} \frac{\partial r}{\partial x} + \frac{\partial w}{\partial \theta} \frac{\partial \theta}{\partial x} \\ &= \frac{\partial w}{\partial r} \cos(\theta) - \frac{\partial w}{\partial \theta} \frac{\sin(\theta)}{r} \end{aligned} \quad (3.10)$$

The evaluation of $\frac{\partial^2 w}{\partial x^2}$ can be performed by taking the derivative of equation (3.10) with respect to x and manipulating.

$$\begin{aligned} \frac{\partial^2 w}{\partial x^2} &= \cos(\theta) \frac{\partial}{\partial r} \left(\frac{\partial w}{\partial x} \right) - \frac{1}{r} \sin(\theta) \frac{\partial}{\partial \theta} \left(\frac{\partial w}{\partial x} \right) \\ &= \frac{\partial^2 w}{\partial r^2} \cos^2(\theta) - 2 \frac{\partial^2 w}{\partial r \partial \theta} \frac{\sin(\theta) \cos(\theta)}{r} + \frac{\partial w}{\partial r} \frac{\sin^2(\theta)}{r} + 2 \frac{\partial w}{\partial \theta} \frac{\sin(\theta) \cos(\theta)}{r^2} \\ &\quad + \frac{\partial^2 w}{\partial \theta^2} \frac{\sin^2(\theta)}{r^2} \end{aligned} \quad (3.11)$$

Similarly

$$\begin{aligned} \frac{\partial^2 w}{\partial y^2} = & \frac{\partial^2 w}{\partial r^2} \sin^2(\theta) + 2 \frac{\partial^2 w}{\partial r \partial \theta} \frac{\sin(\theta) \cos(\theta)}{r} + \frac{\partial w}{\partial r} \frac{\cos^2(\theta)}{r} - 2 \frac{\partial w}{\partial \theta} \frac{\sin(\theta) \cos(\theta)}{r^2} \\ & + \frac{\partial^2 w}{\partial \theta^2} \frac{\cos^2(\theta)}{r^2} \end{aligned} \quad (3.12)$$

$$\begin{aligned} \frac{\partial^2 w}{\partial x \partial y} = & \frac{\partial^2 w}{\partial r^2} \sin(\theta) \cos(\theta) + \frac{\partial^2 w}{\partial r \partial \theta} \frac{\cos(2\theta)}{r} - \frac{\partial w}{\partial \theta} \frac{\cos^2(\theta)}{r^2} - \frac{\partial w}{\partial r} \frac{\sin(\theta) \cos(\theta)}{r} \\ & - \frac{\partial^2 w}{\partial \theta^2} \frac{\sin(\theta) \cos(\theta)}{r^2} \end{aligned} \quad (3.13)$$

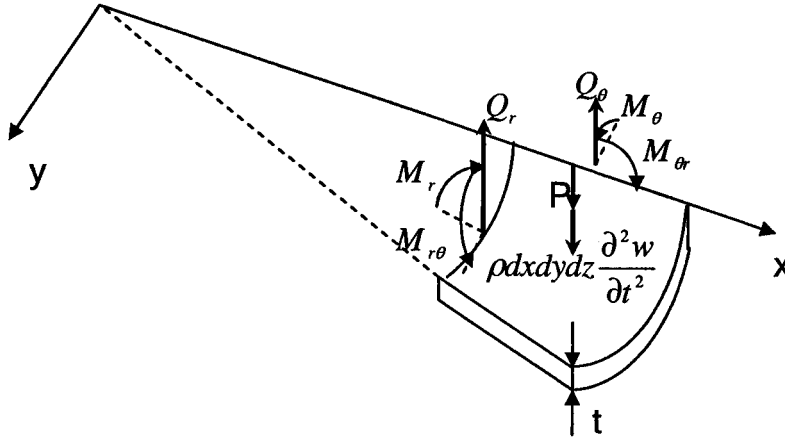


Figure 3.3 Free body diagram of plate element in polar coordinate

As shown in figure 3.3, the free body diagram of a plate in polar coordinates is similar to figure 3.1, but all derivative terms are converted in polar coordinates by applying equation (3.11) through (3.13) into moment equation of the cut plane. The resulting expressions are presented by the following equations

$$M_r = -D \left(\frac{\partial^2 w}{\partial r^2} + \nu \left(\frac{1}{r} \frac{\partial w}{\partial r} + \frac{1}{r^2} \frac{\partial^2 w}{\partial \theta^2} \right) \right) \quad (3.14)$$

$$M_{\theta} = -D \left(\frac{1}{r} \frac{\partial w}{\partial r} + \frac{1}{r^2} \frac{\partial^2 w}{\partial \theta^2} + \nu \frac{\partial^2 w}{\partial r^2} \right) \quad (3.15)$$

$$M_{r\theta} = -D(1-\nu) \left(\frac{1}{r} \frac{\partial^2 w}{\partial r \partial \theta} - \frac{1}{r^2} \frac{\partial w}{\partial \theta} \right) \quad (3.16)$$

And

$$Q_r = -D \frac{\partial}{\partial r} (\nabla^2 w) \quad (3.17)$$

$$\begin{aligned} Q_{\theta} &= -D \frac{\partial}{\partial y} (\nabla^2 w) = -D \frac{\partial}{\partial \theta} (\nabla^2 w) \frac{\partial \theta}{\partial y} \\ &= -D \frac{1}{r} \frac{\partial}{\partial \theta} (\nabla^2 w) \end{aligned} \quad (3.18)$$

The Laplacian operator of surface deflection, w , in rectangular coordinate, it is converted to polar coordinate by solving equation (3.11) and (3.12) for

$\frac{\partial^2 w}{\partial x^2} + \frac{\partial^2 w}{\partial y^2}$ as shown in following equation.

$$\nabla^2 w = \frac{\partial^2 w}{\partial x^2} + \frac{\partial^2 w}{\partial y^2} = \frac{\partial^2 w}{\partial r^2} + \frac{1}{r} \frac{\partial w}{\partial r} + \frac{1}{r^2} \frac{\partial^2 w}{\partial \theta^2}$$

so,
$$\nabla^2 = \frac{\partial^2}{\partial x^2} + \frac{\partial^2}{\partial y^2} = \frac{\partial^2}{\partial r^2} + \frac{1}{r} \frac{\partial}{\partial r} + \frac{1}{r^2} \frac{\partial^2}{\partial \theta^2} \quad (3.19)$$

From equation (3.19), the Bilaplacian operator of rectangular coordinate can be converted to polar coordinate as shown in equation (3.20).

$$\nabla^4 = \nabla^2 \cdot \nabla^2$$

$$\nabla^4 w(x, y) = \nabla^4 w(r, \theta)$$

$$\nabla^4 w(r, \theta) = \left(\frac{\partial^2}{\partial r^2} + \frac{1}{r} \frac{\partial}{\partial r} + \frac{1}{r^2} \frac{\partial^2}{\partial \theta^2} \right) \left(\frac{\partial^2 w}{\partial r^2} + \frac{1}{r} \frac{\partial w}{\partial r} + \frac{1}{r^2} \frac{\partial^2 w}{\partial \theta^2} \right) \quad (3.20)$$

In conclusion, the plate dynamic equation of motion in polar coordinate is

$$\rho h \frac{\partial^2 w}{\partial t^2} = -D \left(\begin{aligned} &\frac{\partial^4 w}{\partial r^4} + \frac{2}{r} \frac{\partial^3 w}{\partial r^3} - \frac{1}{r^2} \frac{\partial^2 w}{\partial r^2} + \frac{2}{r^2} \frac{\partial^2 w}{\partial r \partial \theta} \\ & - \frac{2}{r^3} \frac{\partial^3 w}{\partial r \partial \theta^3} + \frac{4}{r^4} \frac{\partial^2 w}{\partial \theta^2} + \frac{1}{r^3} \frac{\partial w}{\partial r} - \frac{1}{r^4} \frac{\partial^4 w}{\partial \theta^4} \end{aligned} \right) + P \quad (3.21)$$

3.4 Axis Symmetrical Stress Distribution

From the previous section, development of the plate vibration equation is given in general polar coordinates. In this section, the assumption of axis symmetrical bending is employed to yield the deflection of plate only in terms of radial position when the load is symmetrically distributed with respect to center of the plate. For this reason, surface deflection is a function of radius and time, $w(r, t)$, and the moment and shear force expressions of symmetrically loaded plate reduce to equation (3.22) through (3.24).

$$M_r = -D \left(\frac{\partial^2 w}{\partial r^2} + \frac{\nu}{r} \frac{\partial w}{\partial r} \right) \quad (3.22)$$

$$M_\theta = -D \left(\frac{1}{r} \frac{\partial w}{\partial r} + \nu \frac{\partial^2 w}{\partial r^2} \right) \quad (3.23)$$

$$Q_r = -D \frac{\partial}{\partial r} \left(\frac{\partial^2 w}{\partial r^2} + \frac{1}{r} \frac{\partial w}{\partial r} \right) \quad (3.24)$$

Also, the differential equation of the deflection surface becomes

$$-D \left(\frac{\partial^4 w}{\partial r^4} + \frac{2}{r} \frac{\partial^3 w}{\partial r^3} - \frac{1}{r^2} \frac{\partial^2 w}{\partial r^2} + \frac{1}{r^3} \frac{\partial w}{\partial r} \right) + P = \rho h \ddot{w}$$

which can be written in the Bilaplacian operator form as equation (3.25).

$$-D \nabla^4 w + P = \rho h \ddot{w} \quad (3.25)$$

where
$$\nabla^4 w = \frac{\partial^4 w}{\partial r^4} + \frac{2}{r} \frac{\partial^3 w}{\partial r^3} - \frac{1}{r^2} \frac{\partial^2 w}{\partial r^2} + \frac{1}{r^3} \frac{\partial w}{\partial r}$$

The plate equation in (3.25) is thus reduced to one spatial variable accompanied with one time variable, so the resulting plate vibration model is simpler and more convenient.

3.5 Damping Coefficient of Plate

Vibration damping is observed in plate dynamics. It is known that the damping force is proportional to the velocity of plate surface subjected to harmonic excitation, so the damping force term is added to equation (3.25) to create a damped model as shown in equation (3.26).

$$-D\nabla^4 w - c\dot{w} + P = \rho h \ddot{w} \quad (3.26)$$

3.6 Plate Equation under Combined Lateral and In-Plane Loads

In previous discussion, it is assumed that the plate is bent by lateral load only. In conclusion of forces acting in the midplane of the plate has a significant effect on plate bending particularly when large plate bending occurs. Initially, it is assumed that the midsurface is strained by the combined load, so assumption of unstrained midplane is no longer valid. On the other hand, the deflection of plate element is still regarded as small so that the other assumptions are still held. Considering a plate element, strain in figure 3.4, the element is under the action of direct force acting on the midplane.

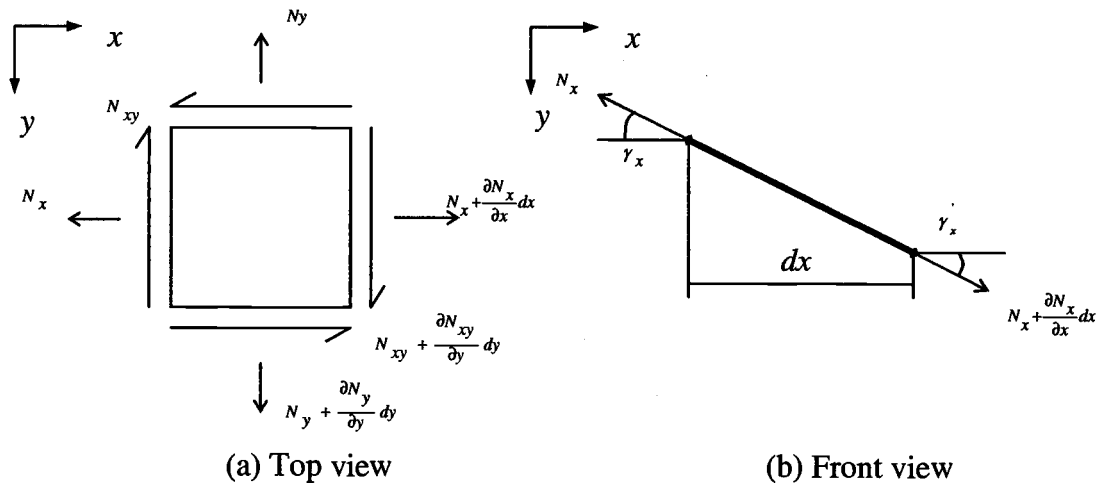


Figure 3.4 Force on the midplane of plate element

From Figure 3.4, the top and front views of an element are shown along with the magnitude of the midplane forces per unit length by N_x ,

N_y and $N_{xy} = N_{yx}$. Projecting these forces on the X and Y-axis, and assuming that there are no body forces yield.

$$\frac{\partial N_x}{\partial x} + \frac{\partial N_{xy}}{\partial y} = 0 \quad (3.27a)$$

$$\frac{\partial N_y}{\partial y} + \frac{\partial N_{xy}}{\partial x} = 0 \quad (3.27b)$$

In considering of the projection of the force on the Z-axis in figure 3.4b, it is necessary to consider the Z components of the in-plane force exerted at each edge of element. The Z component of the normal forces acting on the X-axis is equal to

$$-N_x dy \cdot \sin(\gamma_x) + \left(N_x + \frac{\partial N_x}{\partial x} dx \right) \cdot \sin(\gamma'_x) = 0 \quad (3.28)$$

Assuming small angles for γ_x and γ'_x

$$\sin(\gamma_x) \approx \gamma_x \approx \frac{\partial w}{\partial x}$$

$$\sin(\gamma'_x) \approx \gamma'_x \approx \gamma_x + \frac{\partial \gamma_x}{\partial x} dx = \frac{\partial w}{\partial x} + \frac{\partial^2 w}{\partial x^2} dx$$

Substituting these approximations into equation (3.28), the resulting expression is shown in equation (3.29) as the normal force N_x

$$N_x \frac{\partial^2 w}{\partial x^2} dx dy + \frac{\partial N_x}{\partial x} \frac{\partial w}{\partial x} dx dy = 0 \quad (3.29)$$

Similarly, the Z component of the normal force N_y is obtained as equation (3.30)

$$N_y \frac{\partial^2 w}{\partial y^2} dx dy + \frac{\partial N_y}{\partial y} \frac{\partial w}{\partial y} dx dy = 0 \quad (3.30)$$

Regarding the shear forces N_{xy} on the Z-axis, it can be observed that the slope of deflection surface on the Y direction on two opposite sides of the element on the X edge is $\frac{\partial w}{\partial y}$ and $\frac{\partial w}{\partial y} + \frac{\partial^2 w}{\partial x \partial y} dx$. Hence, the projection of the shear force on Z-axis is then,

$$N_{xy} \frac{\partial^2 w}{\partial x \partial y} dxdy + \frac{\partial N_{xy}}{\partial x} \frac{\partial w}{\partial y} dxdy = 0 \quad (3.31a)$$

An expression identical to the above is found for the Z projection of shear forces N_{yx} acting on the Y edge

$$N_{yx} \frac{\partial^2 w}{\partial x \partial y} dxdy + \frac{\partial N_{yx}}{\partial y} \frac{\partial w}{\partial x} dxdy = 0 \quad (3.31b)$$

As mentioned before, the projections of shear forces acting on X and Y edges are equal to each other, and then the final expression for the projection of all shear forces on Z-axis can be written as equation (3.31c).

$$2N_{xy} \frac{\partial^2 w}{\partial x \partial y} dxdy + \frac{\partial N_{xy}}{\partial x} \frac{\partial w}{\partial y} dxdy + \frac{\partial N_{yx}}{\partial y} \frac{\partial w}{\partial x} dxdy = 0 \quad (3.31c)$$

Adding all of equations (3.31) into equation (3.2), the Dynamic equation of plate becomes

$$\begin{aligned} & \left(\frac{\partial Q_x}{\partial x} + \frac{\partial Q_y}{\partial y} + P \right) + N_x \frac{\partial^2 w}{\partial x^2} + 2N_{xy} \frac{\partial^2 w}{\partial x \partial y} + N_y \frac{\partial^2 w}{\partial y^2} + \left(\frac{\partial N_x}{\partial x} + \frac{\partial N_{xy}}{\partial y} \right) \frac{\partial w}{\partial x} \\ & + \left(\frac{\partial N_y}{\partial y} + \frac{\partial N_{xy}}{\partial x} \right) \frac{\partial w}{\partial y} = \rho h \frac{\partial^2 w}{\partial t^2} \end{aligned}$$

Manipulating the above expression with equation (3.4) and (3.27), the simplified form of dynamic plate equation under the combined action of lateral loads and forces in the midplane can be shown by equation (3.32).

$$\begin{aligned} & -\frac{D}{\rho h} \left(\frac{\partial^4 w}{\partial x^4} + 2 \frac{\partial^4 w}{\partial x^2 \partial y^2} + \frac{\partial^4 w}{\partial y^4} \right) + \frac{1}{\rho h} \left(N_x \frac{\partial^2 w}{\partial x^2} + 2N_{xy} \frac{\partial^2 w}{\partial x \partial y} + N_y \frac{\partial^2 w}{\partial y^2} \right) + \frac{P}{\rho h} = \frac{\partial^2 w}{\partial t^2} \\ & -\frac{D}{\rho h} \nabla^4 w + \frac{1}{\rho h} \left(N_x \frac{\partial^2 w}{\partial x^2} + 2N_{xy} \frac{\partial^2 w}{\partial x \partial y} + N_y \frac{\partial^2 w}{\partial y^2} \right) + \frac{P}{\rho h} = \frac{\partial^2 w}{\partial t^2} \quad (3.32) \end{aligned}$$

In next step, the midplane strain is considered as a source of applied forces acting to midplane element. Referring to total strain on the midplane, it provides relation of the total strain and surface deflection as following.

$$\frac{\partial^2 \varepsilon_x}{\partial y^2} + \frac{\partial^2 \varepsilon_y}{\partial x^2} - \frac{\partial^2 \gamma_{xy}}{\partial x \partial y} = \left(\frac{\partial^2 w}{\partial x \partial y} \right) - \frac{\partial^2 w}{\partial x^2} \frac{\partial^2 w}{\partial y^2}$$

According to Hooke's law, the strain components can be replaced by the equivalent expressions as following

$$\left. \begin{aligned} \varepsilon_x &= \frac{1}{Eh} (N_x - \nu N_y) \\ \varepsilon_y &= \frac{1}{Eh} (N_y - \nu N_x) \\ \gamma_{xy} &= \frac{1}{Gh} N_{xy} \end{aligned} \right\} \quad (3.33)$$

Upon introduction of equations (3.33) into the expressions of strain components on the midplane, the third equation in terms of N_x , N_y and N_{xy} is obtained. The solution of these three equations is simplified by the Airy stress function $\phi(x, y)$, related to in-plane forces as following

$$\left. \begin{aligned} N_x &= h \frac{\partial \phi^2}{\partial y^2} \\ N_y &= h \frac{\partial \phi^2}{\partial x^2} \\ N_{xy} &= -h \frac{\partial \phi^2}{\partial x \partial y} \end{aligned} \right\} \quad (3.34)$$

Substituting equations (3.34) into (3.33), the strain components become

$$\begin{aligned} \varepsilon_x &= \frac{1}{E} \left(\frac{\partial \phi^2}{\partial y^2} - \nu \frac{\partial \phi^2}{\partial x^2} \right) \\ \varepsilon_y &= \frac{1}{E} \left(\frac{\partial \phi^2}{\partial x^2} - \nu \frac{\partial \phi^2}{\partial y^2} \right) \\ \gamma_{xy} &= -\frac{2(1+\nu)}{E} \frac{\partial \phi^2}{\partial x \partial y} \end{aligned}$$

Then, applying above expressions into differential equation of strain component on the midplane, the resulting expression can be shown in equation (3.35).

$$\frac{\partial^4 \phi}{\partial x^4} + 2 \frac{\partial^4 \phi}{\partial x^2 \partial x^2} + \frac{\partial^4 \phi}{\partial y^4} = E \left(\left(\frac{\partial^2 w}{\partial x \partial y} \right)^2 - \frac{\partial^2 w}{\partial x^2} \frac{\partial^2 w}{\partial y^2} \right) \quad (3.35)$$

Substituting equation (3.34) into (3.36)

$$-\frac{D}{\rho h} \nabla^4 w + \frac{1}{\rho} \left(\frac{\partial^2 \phi}{\partial y^2} \frac{\partial^2 w}{\partial x^2} + 2 \frac{\partial^2 \phi}{\partial x \partial y} \frac{\partial^2 w}{\partial x \partial y} + \frac{\partial^2 \phi}{\partial x^2} \frac{\partial^2 w}{\partial y^2} \right) + \frac{P}{\rho h} = \frac{\partial^2 w}{\partial t^2} \quad (3.36)$$

The two above equations are for the general equations for the large deflection of thin plates.

Like the small deflection plate equation, a damping term is appended to these equations.

$$\begin{aligned} \frac{\partial^4 \phi}{\partial x^4} + 2 \frac{\partial^4 \phi}{\partial x^2 \partial x^2} + \frac{\partial^4 \phi}{\partial y^4} &= E \left(\left(\frac{\partial^2 w}{\partial x \partial y} \right)^2 - \frac{\partial^2 w}{\partial x^2} \frac{\partial^2 w}{\partial y^2} \right) \\ -\frac{D}{\rho h} \nabla^4 w + \frac{1}{\rho} \left(\frac{\partial^2 \phi}{\partial y^2} \frac{\partial^2 w}{\partial x^2} + 2 \frac{\partial^2 \phi}{\partial x \partial y} \frac{\partial^2 w}{\partial x \partial y} + \frac{\partial^2 \phi}{\partial x^2} \frac{\partial^2 w}{\partial y^2} \right) - \frac{c}{\rho h} \dot{w} + \frac{P}{\rho h} &= \frac{\partial^2 w}{\partial t^2} \end{aligned} \quad (3.37)$$

The transformation of equation (3.37) from X-Y coordinate to axisymmetric polar coordinate is conducted with equation 3.1, and the resulting expressions of large deflection equation becomes

$$\nabla^4 \phi = -\frac{Eh}{r} (w_r w_{rr}) \quad (3.38a)$$

$$-\frac{D}{\rho h} \nabla^4 w - \frac{c}{\rho h} \dot{w} + \frac{1}{\rho h \cdot r} (\phi_r w_r)_r + \frac{P}{\rho h} = \ddot{w} \quad (3.38b)$$

3.7 Droplet Formation Model

In this project, the droplet prediction is considered as the goal of the work. A one-dimensional numerical model of a droplet is employed. The droplet formation is a function nozzle velocity and chamber pressure. Referring to figure 3.5, a liquid column emerges from a nozzle to form a single droplet. The fundamental derivations of the continuity and momentum equations are based on Adam and Roy [3] for a one-dimensional model of a drop-on-demand inkjet. The model of droplet prediction, developed by Yang [34] is adapted for Adam and Roy.

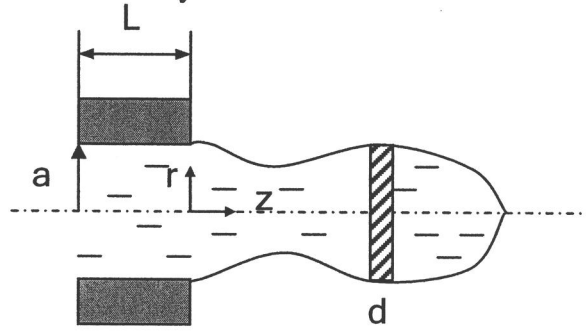


Figure 3.5 Geometry of the liquid column from orifice

Following the derivation in [3] and [34], the continuity and z-direction moment equations are expressed as

$$\frac{\partial u_z}{\partial t} + u_z \cdot \frac{\partial u_z}{\partial z} = \frac{1}{\rho} \cdot \left(-\sigma \cdot \frac{\partial}{\partial z} \left(\frac{1}{R_N} + \frac{1}{R_T} \right) + 3 \cdot \mu \frac{\partial^2 u_z}{\partial z^2} \right) + g_z \quad (3.39)$$

$$\frac{dr_0^2}{dt} + r_0^2 \frac{\partial u_z}{\partial z} + u_z \cdot \frac{\partial r_0^2}{\partial z} = 0 \quad (3.40)$$

where u_r is R-direction absolute velocity, σ is surface tension of water-air, ρ is density of water, μ is the dynamic viscosity of water, and R_N, R_T : principle radii of curvature of the liquid column.

The nondimensional equations of momentum and z-direction continuity for non-moving nozzle become

$$\left. \begin{aligned} \frac{dR^2}{dT} + R^2 \frac{\partial U}{\partial Z} + U \cdot \frac{\partial R^2}{\partial Z} &= 0 \\ \frac{\partial U}{\partial T} + (U) \cdot \frac{\partial U}{\partial Z} &= -\frac{\partial}{\partial Z} \left(\frac{1}{R_N} + \frac{1}{R_T} \right) + 3 \cdot \frac{We}{Re} \cdot \frac{\partial^2 U}{\partial Z^2} + Bo \end{aligned} \right\} \quad (3.41)$$

where $u_c = \sqrt{\frac{\sigma}{\rho \cdot a}}$; $t_c = \sqrt{\frac{\rho \cdot a^3}{\sigma}}$; $u_z = u_c \cdot \hat{U}$; $t = t_c \cdot \hat{T}$; $z = a \cdot \hat{Z}$

$$r_0 = a \cdot \hat{R}_0 ; R_N = a \cdot \hat{R}_N ; R_T = a \cdot \hat{R}_T ; \frac{We}{Re} = \frac{\mu}{\sqrt{\rho \cdot a \cdot \sigma}} ; Bo = \frac{\rho \cdot g_z \cdot a^2}{\sigma}$$

And, the non-dimensional equations of momentum and z-direction continuity for moving nozzle can be expressed by

$$\left. \begin{aligned} \frac{DR}{DT} + \frac{R}{2} \cdot \frac{\partial U_j}{\partial \eta} &= 0 \\ \frac{DU_j}{DT} + \frac{\partial U_o}{\partial T} &= -\frac{\partial}{\partial \eta} \left(\frac{1}{R_N} + \frac{1}{R_T} \right) + 3 \cdot \frac{We}{Re} \cdot \frac{\partial^2 U_j}{\partial \eta^2} + Bo \end{aligned} \right\} \quad (3.42)$$

where $\eta = \hat{Z} - \hat{U}_o \cdot T$ and $\hat{U}_j = \hat{U}_z - \hat{U}_o$

CHAPTER 4

SOLUTIONS OF PLATE EQUATION

In chapter 3, the development of a mathematic model of a thin plate is provided. Since a solution to the differential equations can be generated by either analytical or numerical methods, both methods are implemented in this thesis to verify the solutions. In solving the differential equation with both spatial and temporal variables, initial and boundary conditions must be specified. The initial conditions are assumed that the system is initially at rest as stated below

$$w(r,0) = 0 \quad (4.1a)$$

$$\frac{\partial w(r,t)}{\partial t} \Big|_{t=0} = 0 \quad (4.1b)$$

Generally, the solution of the differential equation, embodied with spatial terms, needs to satisfy the boundary conditions with respect to designated forces or displacement. In this thesis, there are two types of boundary conditions to be satisfied; clamped and free edges.

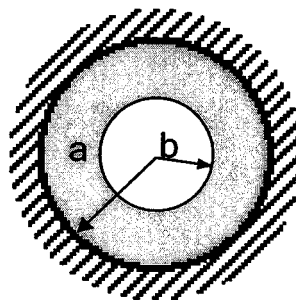


Figure 4.1 Annular clamped plate

At clamped edge:

$$w(a,t) = 0 \quad (4.2a)$$

$$\frac{\partial w(r,t)}{\partial r} \Big|_{r=a} = 0 \quad (4.2b)$$

Free edge such as the inner side is free of moment along the radial axis and vertical shear force, so the differential terms for symmetrical bending can be derived from equation (3.22) through (3.24) with the conditions of $M_r = 0$ and $V_r = Q_r = 0$. The resulting expression is given by equations (4.3).

$$M_r = 0; \quad -D \left(\frac{\partial^2 w}{\partial r^2} + \frac{\nu}{r} \frac{\partial w}{\partial r} \right) = 0 \quad (4.3a)$$

$$Q_r = 0; \quad -D \left(\frac{\partial^3 w}{\partial r^3} + \frac{1}{r} \frac{\partial^2 w}{\partial r^2} - \frac{1}{r^2} \frac{\partial w}{\partial r} \right) = 0 \quad (4.3b)$$

According to the introduction of Airy stress function in equation (3.38), the additional boundary conditions for $\phi(r,t)$ are necessary for solving the governing equation for large deflection. The development of boundary conditions of the stress function originated from the total strain component. The X-Y strain components are known from Urugal[28], so the transformation of these terms into polar coordinates is

$$\left. \begin{aligned} \varepsilon_r &= \frac{\partial u}{\partial r} + \frac{1}{2} \left(\frac{\partial w}{\partial r} \right)^2 \\ \varepsilon_\theta &= \frac{u}{r} \end{aligned} \right\} \quad (4.4)$$

where u denotes the displacement in radial axis

Denoting the corresponding tensile forces by N_r and N_θ , and applying Hooke's law, the strain components and tensile forces can be related as follows;

$$\left. \begin{aligned} \varepsilon_r &= \frac{1}{Eh} (N_r - \nu N_\theta) \\ \varepsilon_\theta &= \frac{1}{Eh} (N_\theta - \nu N_r) \end{aligned} \right\} \quad (4.5)$$

The relation between tensile forces and the stress function are needed. The relations between tensile forces and stress function are defined as shown in equation 4.6.

$$\left. \begin{aligned} N_r &= \frac{1}{r} F_r \\ N_\theta &= F_{rr} \end{aligned} \right\} \quad (4.6)$$

The trivial definition for the clamped edge boundary condition is

$$\begin{aligned} w &= 0 & \frac{\partial w}{\partial r} &= 0 \\ \varepsilon_r &= 0 & \varepsilon_\theta &= 0 \\ u &= 0 \end{aligned}$$

Then, from equations (4.4) for ε_θ , it's evident that ε_θ is zero at clamped edge. Applying condition $\varepsilon_\theta = 0$ and manipulating the whole term with equation (4.6), the resulting expression becomes

$$\frac{\nu}{r} \phi_r = \phi_{rr} \quad (4.7)$$

There is no stress occurred along the radial axis at the free edge, so it is apparent that

$$N_r = \phi_r = 0 \quad (4.8)$$

4.1 Analytical Solutions of Clamped Annular Plate

In this section, the separated variable method is brought to tackle the problem where the solution is in the terms of mode shape and function of time. This part is started with free vibration solution and followed by force vibration solution of clamped annular plate.

4.1.1 Free Vibration Solutions of Clamped Annular Plate

Consider the equation (3.26) excluding the excitation as the model.

$$D\nabla^4 w + c\dot{w} + \rho h\ddot{w} = 0 \quad (4.9)$$

To solve this equation, the separation of variables will be employed by assuming a solution of the form given in equation (4.10).

$$w(r,t) = H(r)G(t) \quad (4.10)$$

Applying the separated solution into equation (4.9) and manipulating, it gives

$$\nabla^4 H(r) - \beta^4 H(r) = 0 \quad (4.11)$$

$$\ddot{G}(t) + \frac{c}{\rho h} \dot{G}(t) + \frac{\beta^4 D}{\rho h} G(t) = 0 \quad (4.12)$$

According to the shape of nozzle plate, it is considered as a clamped annular plate. The inner edge is subjected to free-edge boundary condition in which mode shape must satisfy the conditions also. The solution of spatial differential equation is in Bessel function form as

$$H_i(r) = A_i J_0(\beta_i r) + E_i Y_0(\beta_i r) + B_i I_0(\beta_i r) + F_i K_0(\beta_i r) \quad (4.13)$$

From above equation, it needs to satisfy all of 4 boundary conditions as the following terms

At outer clamped edge with radius a

$$H_i(a) = 0$$

$$H_i'(a) = 0$$

At inner free edge with radius b

$$M_r(b) = 0 \quad ; \quad -D \left(\frac{\partial^2 w}{\partial r^2} + \frac{v}{r} \frac{\partial w}{\partial r} \right)_{r=b} = 0$$

$$Q_r(b) = 0 \quad ; \quad -D \left(\frac{\partial^3 w}{\partial r^3} + \frac{1}{r} \frac{\partial^2 w}{\partial r^2} - \frac{1}{r^2} \frac{\partial w}{\partial r} \right) = 0$$

Applying above 4 equations to equation (4.13), the resulting terms are shown by equations (4.14).

$$A_i J_0(\beta_i a) + E_i Y_0(\beta_i a) + B_i I_0(\beta_i a) + F_i K_0(\beta_i a) = 0 \quad (4.14a)$$

$$-A_i \beta_i J_1(\beta_i a) - E_i \beta_i Y_1(\beta_i a) - B_i \beta_i I_1(\beta_i a) - F_i \beta_i K_1(\beta_i a) = 0 \quad (4.14b)$$

$$\begin{aligned}
& -\frac{A_i \beta_i}{b} (\beta_i b J_0(\beta_i b) - (1-\nu) J_1(\beta_i b)) + \frac{B_i \beta_i}{b} (\beta_i b I_0(\beta_i b) - (1-\nu) I_1(\beta_i b)) \\
& -\frac{E_i \beta_i}{b} (\beta_i b Y_0(\beta_i b) - (1-\nu) Y_1(\beta_i b)) + \frac{A_i \beta_i}{b} (\beta_i b K_0(\beta_i b) - (1-\nu) K_1(\beta_i b)) \\
& = 0
\end{aligned} \tag{4.14c}$$

$$A_i \beta_i^3 J_1(\beta_i b) + E_i \beta_i^3 Y_1(\beta_i b) + B_i \beta_i^3 I_1(\beta_i b) - F_i \beta_i^3 K_1(\beta_i b) = 0 \tag{4.14d}$$

All above Bessel expressions can be simplified and put into the matrix form as following equation (4.15).

$$\left[\begin{array}{c} A_f \end{array} \right] \left[\begin{array}{c} A_i \\ E_i \\ B_i \\ F_i \end{array} \right] = \left[\begin{array}{c} 0 \\ 0 \\ 0 \\ 0 \end{array} \right] \tag{4.15}$$

where

$$[A_f] = \left[\begin{array}{cccc} J_0(\beta_i a) & Y_0(\beta_i a) & I_0(\beta_i a) & K_0(\beta_i a) \\ -J_1(\beta_i a) & -Y_1(\beta_i a) & I_1(\beta_i a) & K_1(\beta_i a) \\ J_{01} & Y_{01} & I_{01} & K_{01} \\ J_1(\beta_i b) & Y_1(\beta_i b) & I_1(\beta_i b) & -K_1(\beta_i b) \end{array} \right]$$

$$\text{and } J_{01} = -J_0(\beta_i b) + \frac{1-\nu}{\beta_i b} J_1(\beta_i b)$$

$$Y_{01} = -Y_0(\beta_i b) + \frac{1-\nu}{\beta_i b} Y_1(\beta_i b)$$

$$I_{01} = I_0(\beta_i b) - \frac{1-\nu}{\beta_i b} I_1(\beta_i b)$$

$$K_{01} = K_0(\beta_i b) + \frac{1-\nu}{\beta_i b} K_1(\beta_i b)$$

From equation (4.15), the roots of determinant of $[A_f]$ are the eigenfrequencies at one specific ratio of inner edge diameter to the outer, α .

$$\alpha = \frac{b}{a}$$

For instance, the dimension of plate are given by

$$b = 0.00005 \text{ m}$$

$$a = 0.004 \text{ m}$$

then

$$\alpha = 0.0125$$

Thus, the first five eigenfrequencies are shown in table 4.1

N th root	Eigenfrequencies
$\beta_0 a$	3.195818
$\beta_1 a$	6.304064
$\beta_2 a$	9.434453
$\beta_3 a$	12.568582
$\beta_4 a$	15.703831

Table 4.1 the eigenfrequencies of $[A_i]$

The coefficients A_i , B_i , E_i and F_i in equation (4.13) are constant to be evaluated by using the minor of $[A_i]$ to normalize each coefficient. The norms of all 4 parameters are shown as follows

$$A_i = \begin{bmatrix} Y_0(\beta_i a) & I_0(\beta_i a) & -K_0(\beta_i a) \\ -Y_1(\beta_i a) & I_1(\beta_i a) & K_1(\beta_i a) \\ Y_{01} & I_{01} & -K_{01} \end{bmatrix} \quad (4.16a)$$

$$E_i = \begin{bmatrix} J_0(\beta_i a) & I_0(\beta_i a) & K_0(\beta_i a) \\ -J_1(\beta_i a) & I_1(\beta_i a) & -K_1(\beta_i a) \\ J_{01} & I_{01} & K_{01} \end{bmatrix} \quad (4.16b)$$

$$B_i = \begin{bmatrix} J_0(\beta_i a) & Y_0(\beta_i a) & -K_0(\beta_i a) \\ -J_1(\beta_i a) & -Y_1(\beta_i a) & K_1(\beta_i a) \\ J_{01} & Y_{01} & -K_{01} \end{bmatrix} \quad (4.16c)$$

$$F_i = \begin{bmatrix} J_0(\beta_i a) & Y_0(\beta_i a) & I_0(\beta_i a) \\ -J_1(\beta_i a) & -Y_1(\beta_i a) & I_1(\beta_i a) \\ J_{01} & Y_{01} & I_{01} \end{bmatrix} \quad (4.16d)$$

Obviously, the normalized mode shape is derived by substituting equations (4.16) into (4.13), but the general mode shape of annular plate requires the orthogonality to satisfy Fourier series solution. So, the corresponding mode shape is given by equation (4.17).

$$H_i(r) = \Omega_i (A_i J_0(\beta_i r) + E_i Y_0(\beta_i r) + B_i I_0(\beta_i r) + F_i K_0(\beta_i r)) \quad (4.17)$$

where Ω_i is the orthogonality factor to orthogonalize the normalized mode shape to the corresponding mode shape. Therefore, the orthogonal mode shape can be obtained by manipulating the following equation for Ω_i .

$$\int_b^a \int_0^{2\pi} \rho h \Omega_i^2 [A_i J_0(\beta_i r) + E_i Y_0(\beta_i r) + B_i I_0(\beta_i r) + F_i K_0(\beta_i r)]^2 r dr d\theta = 1$$

$$\text{then } \Omega_i = \sqrt{\frac{1}{2\pi \rho h \int_b^a [A_i J_0(\beta_i r) + E_i Y_0(\beta_i r) + B_i I_0(\beta_i r) + F_i K_0(\beta_i r)]^2 r dr}}$$

4.1.2 Forced Vibration Solutions of Clamped Annular Plate

Considering time derivative terms, the differential temporal equation for force vibration are defined in equation (4.12).

$$\ddot{G}_i(t) + 2\xi\omega_n \dot{G}_i(t) + \omega_n^2 G_i(t) = f_i(t)$$

Determining modal force amplitude with $F(t) = F_0 \cos(\omega t)$

$$\begin{aligned} f_i(t) &= F(t) \iint H_i(r) r dA \\ &= H_{ci} \cos(\omega t) \end{aligned}$$

where $H_{ci} = F_0 \iint H_i(r) r dA$

As a result, the time derivative terms of annular plate can be solved in second order differential form. The solution is shown by equation (4.18).

$$G_i(t) = \frac{H_{ci} e^{-\xi_i \omega_{ni} t}}{(\omega_{ni}^2 - \omega^2)^2 + (2\xi_i \omega_{ni})^2} \left(\begin{aligned} & -(\omega_{ni}^2 - \omega^2) \cos(\omega_{di} t) \\ & + \left(-\frac{\xi_i \omega_{ni}}{\omega_{di}} (\omega_{ni}^2 - \omega^2) - \frac{2\xi_i \omega_{ni} \omega^2}{\omega_{di}} \right) \sin(\omega_{di} t) \end{aligned} \right) \\ + \frac{H_{ci} e^{-\xi_i \omega_{ni} t}}{(\omega_{ni}^2 - \omega^2)^2 + (2\xi_i \omega_{ni})^2} \left((\omega_{ni}^2 - \omega^2) \cos(\omega t) + 2\xi_i \omega_{ni} \omega \sin(\omega t) \right) \quad (4.18)$$

Ultimately, the general solution of annular plate excited by harmonic function, $F_0 \cos(\omega t)$, is based on equation (4.17) and (4.18) as given by equation (4.19).

$$w(r,t) = \sum_{i=1}^{\infty} (H_i(r) G_i(t)) \\ = \sum_{i=1}^{\infty} \left(\begin{aligned} & \frac{\Omega_i H_{ci}}{(\omega_{ni}^2 - \omega^2)^2 + (2\xi_i \omega_{ni})^2} (A_i J_0(\beta_i r) + E_i Y_0(\beta_i r) + B_i I_0(\beta_i r) + F_i K_0(\beta_i r)) \\ & \times \left(\begin{aligned} & e^{-\xi_i \omega_{ni} t} \left(-(\omega_{ni}^2 - \omega^2) \cos(\omega_{di} t) - \frac{\xi_i \omega_{ni}}{\omega_{di}} (\omega_{ni}^2 - \omega^2) \sin(\omega_{di} t) \right) \\ & + (\omega_{ni}^2 - \omega^2) \cos(\omega t) + 2\xi_i \omega_{ni} \omega \sin(\omega t) \end{aligned} \right) \end{aligned} \right) \quad (4.19)$$

$$\text{where } \Omega_i = \frac{1}{\sqrt{2\pi\rho h \int_b^a [A_i J_0(\beta_i r) + E_i Y_0(\beta_i r) + B_i I_0(\beta_i r) + F_i K_0(\beta_i r)]^2 r dr d\theta}}$$

$$H_{ci} = F_0 \iint H_i(r) r dA$$

and A_i, B_i, E_i, F_i are defined in equation (4.16).

4.2 Numerical Solutions of Large Deflection Plate Equation

For solution of the large deflection plate vibration equation, the Galerkin's method is used. This method identifies the governing differential equation of the system subjected to boundary conditions given by various line integrals. The usual way of obtaining the solution of the system for an extremum condition is to solve the differential equation with corresponding boundary conditions. So, the initial step of solving the equation is to define the approximate solution by

$$\tilde{w} = w + \epsilon$$

For the differential equation,

$$Lw(x, y) = 0$$

where L is a differential operator

From above approximate solution of w , it needs to satisfy all boundary conditions (making all the line integrals zero) and obtain the error in the differential equation.

$$\epsilon = L\tilde{w}(x, y)$$

In order to satisfy orthogonality, it requires

$$\iint_R [L\tilde{w}(x, y)]\eta(x, y) dx dy = 0$$

In Galerkin's method, the function $\eta(x, y)$ is chosen as the assumed shape function itself.

$$\iint_R [L\tilde{w}(x, y)]\tilde{w}(x, y) dx dy = 0$$

The approximate solution of annular plate is determined in this section. The expressions of boundary conditions for free edge of annular plate are considered as spatial boundary condition and equation (4.8) is for boundary

condition of stress function. Then, the starting step to reach the solution in separation variable form is shown as follows

$$w(r,t) = H(r)G(t)$$

Also, the approximate shape function is mentioned in Urugal [28]

$$H(r) = 1 + c_1 r^2 + c_2 r^4 + c_3 \ln(r) + c_4 r^2 \ln(r)$$

From above function, there are 4 unknown constants, which need to satisfy the following boundary conditions.

$$w(a,t) = 0$$

$$\frac{\partial w(r,t)}{\partial r} \Big|_{r=a} = 0$$

$$-D \left(\frac{\partial^2 w}{\partial r^2} + \frac{\nu}{r} \frac{\partial w}{\partial r} \right) \Big|_{r=b} = 0$$

$$-D \left(\frac{\partial^3 w}{\partial r^3} + \frac{1}{r} \frac{\partial^2 w}{\partial r^2} - \frac{1}{r^2} \frac{\partial w}{\partial r} \right) \Big|_{r=b} = 0$$

where a is outer radius and b is inner radius.

Applying all above boundary conditions into shape function and solving for all 4 unknown constants, the value of these constants can be solved from the following equations.

$$1 + c_1 a^2 + c_2 a^4 + c_3 \ln(a) + c_4 a^2 \ln(a) = 0$$

$$2c_1 a + 4c_2 a^3 + \frac{c_3}{a} + c_4 a + 2c_4 \ln(a) = 0$$

$$2c_1 + 12b^2 c_2 - \frac{c_3}{b^2} + 3c_4 + 2\ln(b)c_4 + \frac{\nu(2bc_1 + 4b^3 c_2 + \frac{c_3}{b} + bc_4 + 2bc_4 \ln(b))}{b} = 0$$

$$24bc_2 + \frac{2c_3}{b^3} + \frac{2c_4}{b} + \frac{2c_1 + 12b^2c_2 - \frac{c_3}{b^2} + 3c_4 + 2c_4 \ln(b)}{b} - \frac{2bc_1 + 4b^3c_2 - \frac{c_3}{b} + bc_4}{b^2} + \frac{2bc_4 \ln(b)}{b^2} = 0$$

After getting the value of c_1, c_2, c_3 and c_4 , and substituting all above constants into shape function, the closed form solution of shape function can be presented by

$$H_{\text{annular}}(r) = 1 + c_1 r^2 + c_2 r^4 + c_3 \ln(r) + c_4 r^2 \ln(r) \quad (4.20)$$

Then, applying equation (4.10) and (4.20) into (3.38a), the resulting equation is

$$\frac{1}{r} \frac{\partial}{\partial r} \left(r \frac{\partial}{\partial r} \left(\frac{1}{r} \frac{\partial}{\partial r} \left(r \frac{\partial \phi}{\partial r} \right) \right) \right) = -\frac{EhG(t)^2}{r^3} (c_3 + r^2(2c_1 + c_4 + 4c_2 r^2) + 2c_4 r^2 \ln(r)) \cdot \begin{pmatrix} -c_3 + r^2(2c_1 + 3c_4 + 12c_2 r^2) \\ + 2c_4 r^2 \ln(r) \end{pmatrix}$$

Integrating the above, it gives

$$\begin{aligned} \phi(r) = & \frac{3}{8} c_3 c_4 r^2 + \frac{1}{128} (8c_1^2 + 16c_2 c_3 - 8c_1 c_4 + 5c_4^2) r^4 + \frac{1}{16} r^2 (-2c_3^2 + 4c_3 c_4 r^2 + c_4^2 r^4) \ln(r)^2 \\ & + \frac{1}{144} c_4 r^2 (-72c_3 + 18c_1 r^2 - 9c_4 r^2 + 8c_2 r^4) \ln(r) + \frac{1}{216} c_2 (12c_1 - c_4) r^6 + \frac{c_2^2 r^8}{48} \\ & + c_5 \ln(r) + c_6 r^2 \end{aligned} \quad (4.21)$$

where the constants of c_5 and c_6 are to be determined from boundary conditions in equation (4.7) and (4.8). Then, the value of both constants, c_5 and c_6 , can be determined from both of following equations.

$$\begin{aligned} & \frac{b^3 c_1^2}{4} + \frac{1}{3} b^5 c_1 c_2 + \frac{b^7 c_2^2}{6} + \frac{1}{2} b^3 c_2 c_3 - \frac{1}{8} b^3 c_1 c_4 + \frac{1}{36} b^5 c_2 c_4 + \frac{bc_3 c_4}{4} + \frac{3b^3 c_4^2}{32} + \frac{c_5}{b} + 2bc_6 - \frac{c_3^2 \ln(b)}{4b} \\ & + \frac{1}{2} b^3 c_1 c_4 \ln(b) + \frac{1}{3} b^5 c_2 c_4 \ln(b) - \frac{1}{2} bc_3 c_4 \ln(b) - \frac{1}{8} b^3 c_4^2 \ln(b) + \frac{1}{2} bc_3 c_4 \ln(b)^2 + \frac{1}{4} b^3 c_4^2 \ln(b)^2 = 0 \end{aligned}$$

$$\begin{aligned}
& 8a^6 c_2 \left(\begin{array}{l} c_4(-17+\nu) \\ +12c_4(-5+\nu) \end{array} \right) + 48a^8 c_2^2(-7+\nu) + 72a^2 \left(\begin{array}{l} 8c_6(-1+\nu) \\ +c_3c_4(1+\nu) \end{array} \right) + 72a^4 c_4 \left(\begin{array}{l} a^2 c_4(-3+\nu) \\ +2c_3(-1+\nu) \end{array} \right) \ln(a)^2 \\
& + 9a^4 \left(\begin{array}{l} (-3+\nu)(8c_1^2+16c_2c_3) \\ -4c_1c_4(1+\nu)+c_4^2(-5+3\nu) \end{array} \right) - 12 \left(\begin{array}{l} 12a^2 c_3c_4(1+\nu)+a^4 c_4(-8a^2 c_2(-5+\nu)) \\ -12c_1(-3+\nu)+3c_4(1+\nu)+6c_3^2(1+\nu) \end{array} \right) \ln(a) \\
& + 72(c_3^2+4c_5(1+\nu))=0
\end{aligned}$$

So far, all expressions, which are counted for the approximate solutions, are determined. In next step, equation (4.20) and (4.21) are applied to equation (3.38b), and then the error in the differential equation is defined by the following terms.

$$\epsilon = \frac{D}{\rho h} G(t) \nabla^4 \phi(r) + \ddot{G}(t) \phi(r) + \frac{c}{\rho h} \dot{G}(t) \phi(r) + \frac{EhG^3(t)}{\rho h} \frac{1}{r} (\phi_r H_{annular r})_r - \frac{P}{\rho h}$$

Orthogonalizing the above error with assumed shape function, it gives

$$\begin{aligned}
& \frac{D}{\rho h} G(t) \int_b^a (\nabla^4 \phi(r)) \phi(r) \cdot r dr + \ddot{G}(t) \int_b^a \phi^2(r) \cdot r dr + \frac{c}{\rho h} \dot{G}(t) \int_b^a \phi^2(r) \cdot r dr \\
& + \frac{EhG^3(t)}{\rho h a^4} \int_b^a \frac{1}{r} (\phi_r H_{annular r})_r \phi(r) \cdot r dr = \frac{P}{\rho h} \int_b^a \phi(r) \cdot r dr
\end{aligned}$$

Also, replacing Bilaplacian term with the expression in equation (4.11), the nonlinear differential equation for time variable term is presented by

$$\frac{D}{\rho h} \mu \beta_i^4 G(t) + \mu \ddot{G}(t) + \frac{c}{\rho h} \mu \dot{G}(t) + \frac{Eh\psi_{annular}}{a^4} G^3(t) = Q \quad (4.22)$$

where

$$\mu = \int_0^a \phi^2(r) \cdot r dr$$

$$\psi_{annular} = \int_b^a \frac{1}{r} (\phi_r H_{annular r})_r \phi(r) \cdot r dr$$

$$Q(t) = \int_0^a P(t) \cdot \phi(r) \cdot r dr$$

From (4.22), the solutions of $G(t)$ can be determined by using phase variable to transform this equation into state space form and numerically integrating with Runge-Kutta fourth order numerical method.

Finally, the approximate solution of surface deflection of annular plate can be reached by the summation of the product of equation (4.20) and (4.22) at each eigenfrequency.

$$w(r,t) = \sum_{i=1}^{\infty} (H_i(r)G_i(t))$$

where i is the number of mode shape.

CHAPTER 5 RESULTS

Chapter 5 presents the solutions of small deflection and large deflection plate equation. The annular plate model was used in the finding of both linear and nonlinear plate equations. In presenting solutions of the annular plate, this chapter demonstrates the response of the inner edge in accordance to the change in time. The chapter also presents the result of the whole response of annular plate in 3D plotting. The simulation result of integration between plate vibration and droplet formation is also presented in the chapter. Trade studies between Young modulus and Droplet formation characteristic are covered in this chapter. There are three droplet formation characteristics consider in the performing of related simulations.

5.1 Surface Deflection of Small Deflection Plate Equation

In this section, a clamped annular plate is introduced to the simulation. In solving thin plate equation as mentioned earlier, the analytical solutions are available for the linear equation; on the other hand, numerical solutions are available for nonlinear equation. On the theoretical basis, material properties of annular plate are assumed by the following variables.

$$\begin{aligned}
 a &= 0.004 \quad m & b &= 0.00005 \quad m \\
 \rho &= 7590 \quad \frac{kg}{m^3} & h &= 0.000016 \quad m \\
 \nu &= \frac{1}{3} & E &= 102 \text{ GPa} & \zeta &= 1 \%
 \end{aligned}$$

Plate equation 3.25 is the fundamental equation, which is originated from the stress and strain components on the midplane of plate without damping term. However the response of undamped model is not compatible with the physical aspect of plate vibration as shown in figure 5.1.

Figure 5.1 Comparison of damped and undamped solutions of inner node deflection of annular plate.

For this reasoning, the modal damping is added to equation (3.25), and the resulting expression is presented in equation (3.26). It is not possible to determine the damping ratio of the plate directly from datasheet of material properties; therefore, one percentage of damping ratio is approximated into the model. Finally, the actual damping will be determined by a trial-error method with the experimental data.

5.2 Surface deflection of Large Deflection Plate Equation

According to chapter 4, the expressions for solutions of large deflection plate equations are determined by using Galerkin's Method. In this session, the simulation of these solutions is presented along with the verification which was previously conducted by another method such as the Energy method.

For the purpose of comparing the solutions of large deflection, the solutions of the Energy method [28] are used. Referring to [28], the Energy method's approximate solution of maximum deflection for clamped plate can be determined by the use of equation 5.1.

$$w_{\max} = \frac{Pa^4}{64D} \left(1 + 0.488 \left(\frac{w_{\max}}{h} \right)^2 \right) \quad (5.1)$$

where P is the constant pressure acting on the plate.

Then, the simulation of maximum surface deflection can be done by using the constant amplitude force instead of sinusoidal function. Result of both solutions from Energy method and Galerkin's method are presented in figure 5.2.

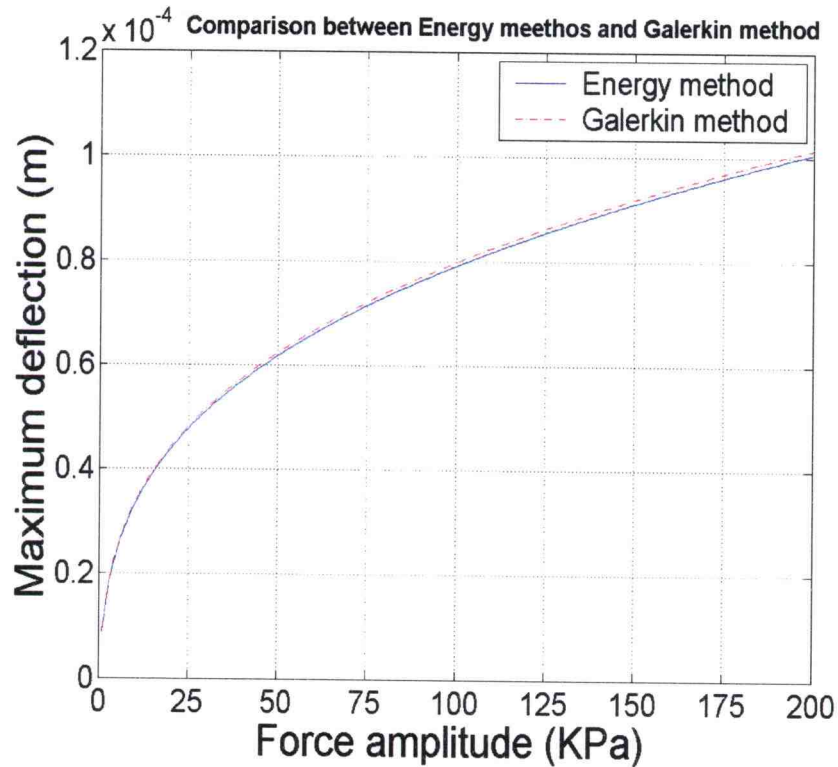


Figure 5.2 Comparison of maximum deflection between Energy method and Galerkin method.

The most appropriate model for plate vibration is expressed in this section, which considers the nozzle plate as annular plate governed by large deflection plate equation. The inner edge node is used to verify the solutions of annular plate vibration. First, the simulation is performed with the small force amplitude of 1 Pa, and then the high amplitude pressure is to be applied to the annular plate. The resulting excitation is shown in figure 5.3.

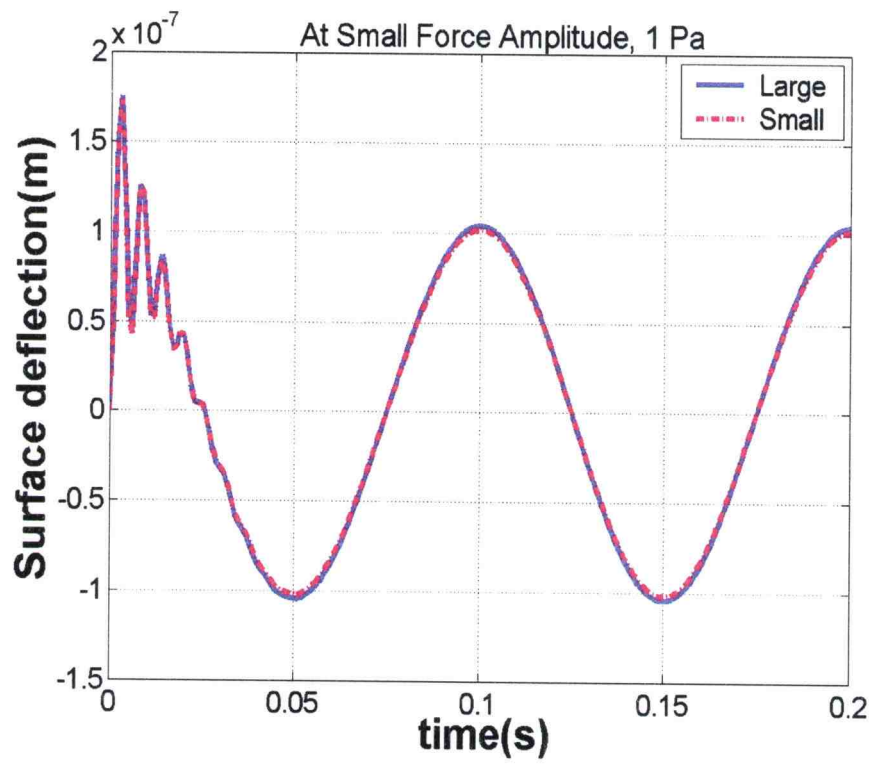


Figure 5.3a Comparison between Small and Large deflection at 1 Pa Force amplitude.

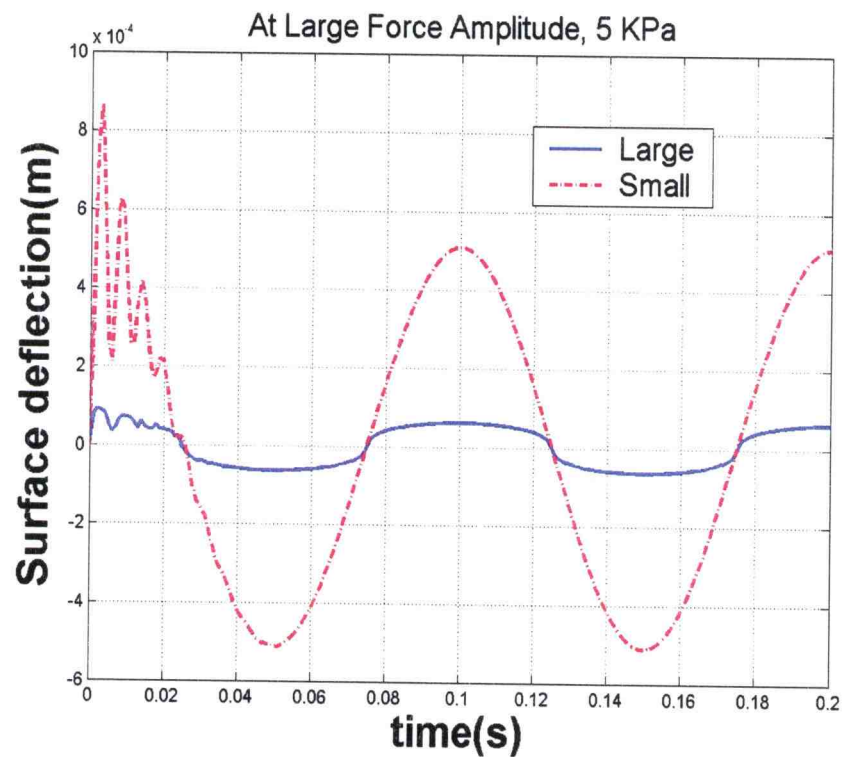


Figure 5.3b Comparison between Small and Large deflection at 5 KPa Force amplitude.

5.3 Droplet formation simulation

The related model of droplet formation simulation is presented in figure 5.4, where the external force excitation is applied at the lower diaphragm. Also, it is assumed that movement of fluid inside the chamber causes the excitation at the upper nozzle plate. With this reasoning in mind, it is reasonable to assume that types of forcing functions applied to diaphragm have a great deal of effect not only to the liquid inside the chamber, but also to the vibration of plate. According to the model, the assumptions of incompressible fluid and uniform pressure distribution in fluid inside the chamber are made in order to estimate the pressure directly actuated to the plate. For the reason of simplification purposes, this thesis employed water as

liquid material in the chamber. Hence, force amplitude of plate excitation is determined by the fluid pressure in the chamber, which is measured by the pressure probe on the top.

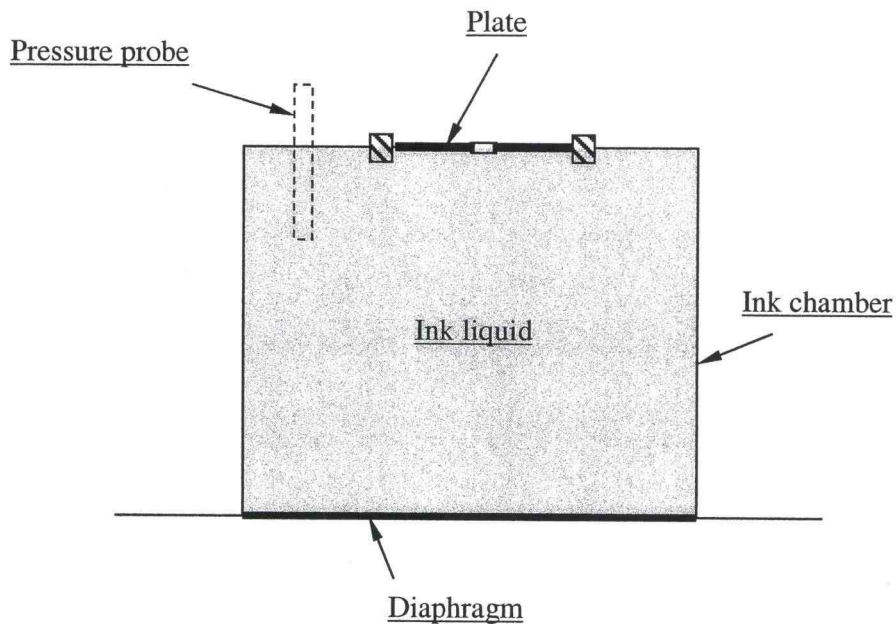


Figure 5.4 Experimental model of Plate vibration

There are 2 parts to the simulation. The first part governs over the formation of droplet under the non-moving nozzle, and the second part focuses on plate vibration solution to predict the droplet with the moving nozzle. The work on the droplet formation computation code is completed which was done to use as aid in the prediction of the first droplet formation produced at nozzle.

Next, the impulse input function is introduced as the excitation force as in figure 5.5.

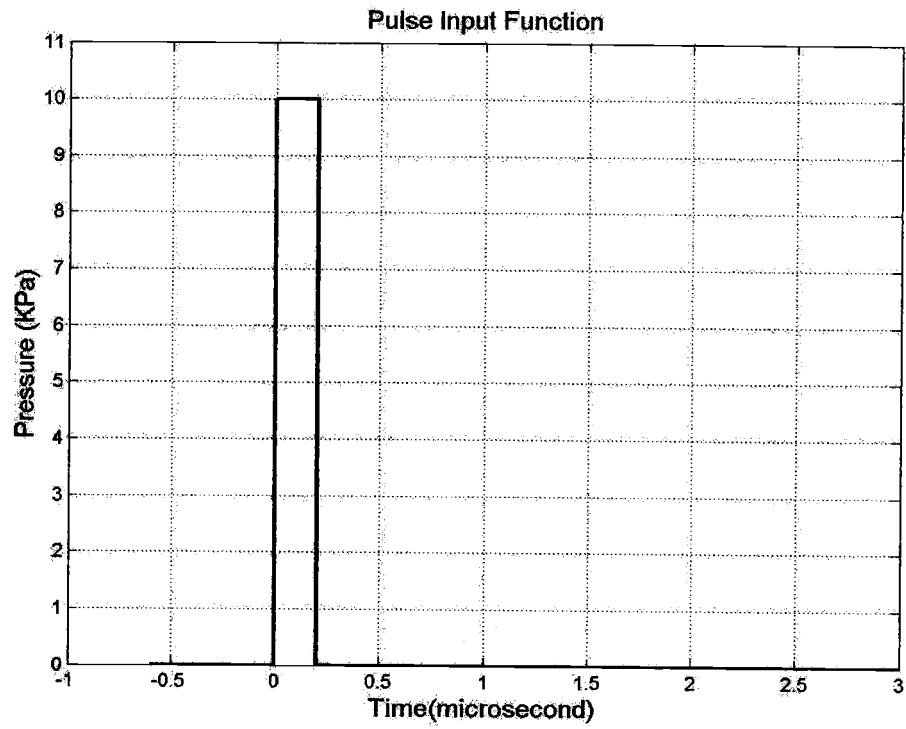


Figure 5.5 Pulse Input Excitation

According to the result from mentioned simulation, the prediction of liquid column shape can be performed by the solving the equation 3.43 by Yang [34]. The result of simulation is presented in figures 5.6.

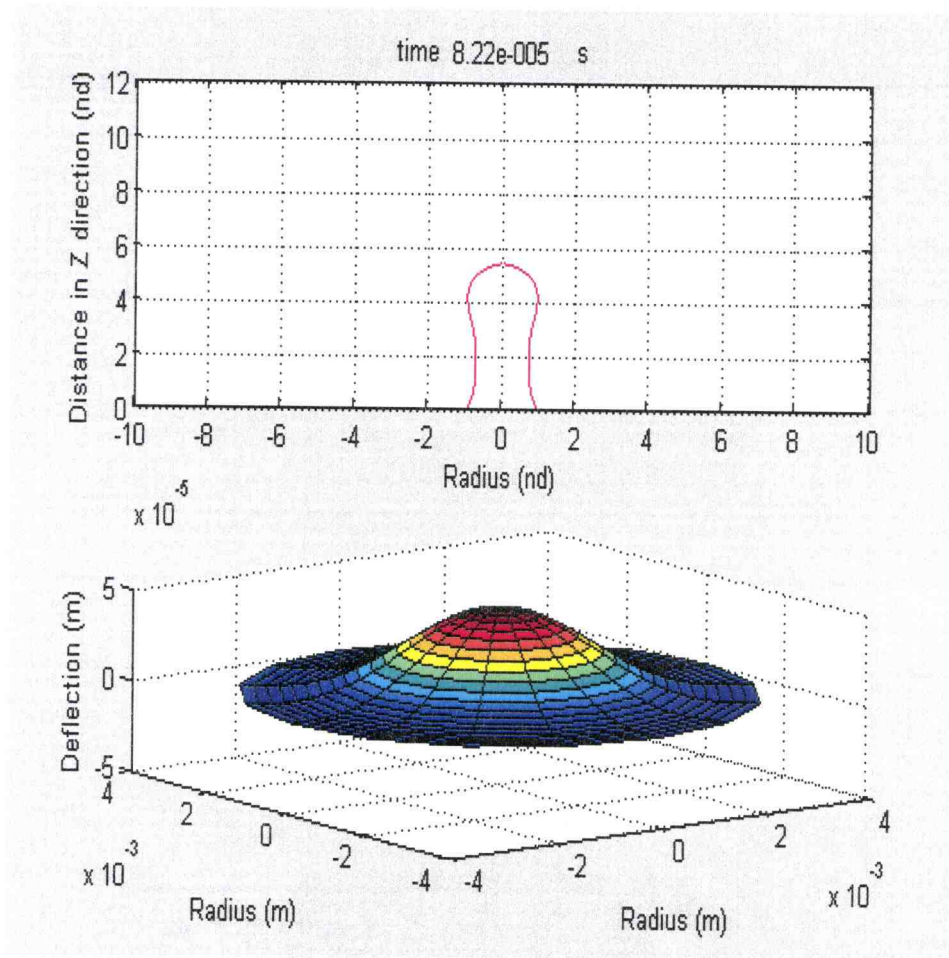


Figure 5.6a Liquid column shape at $t = 0.0000822$ s

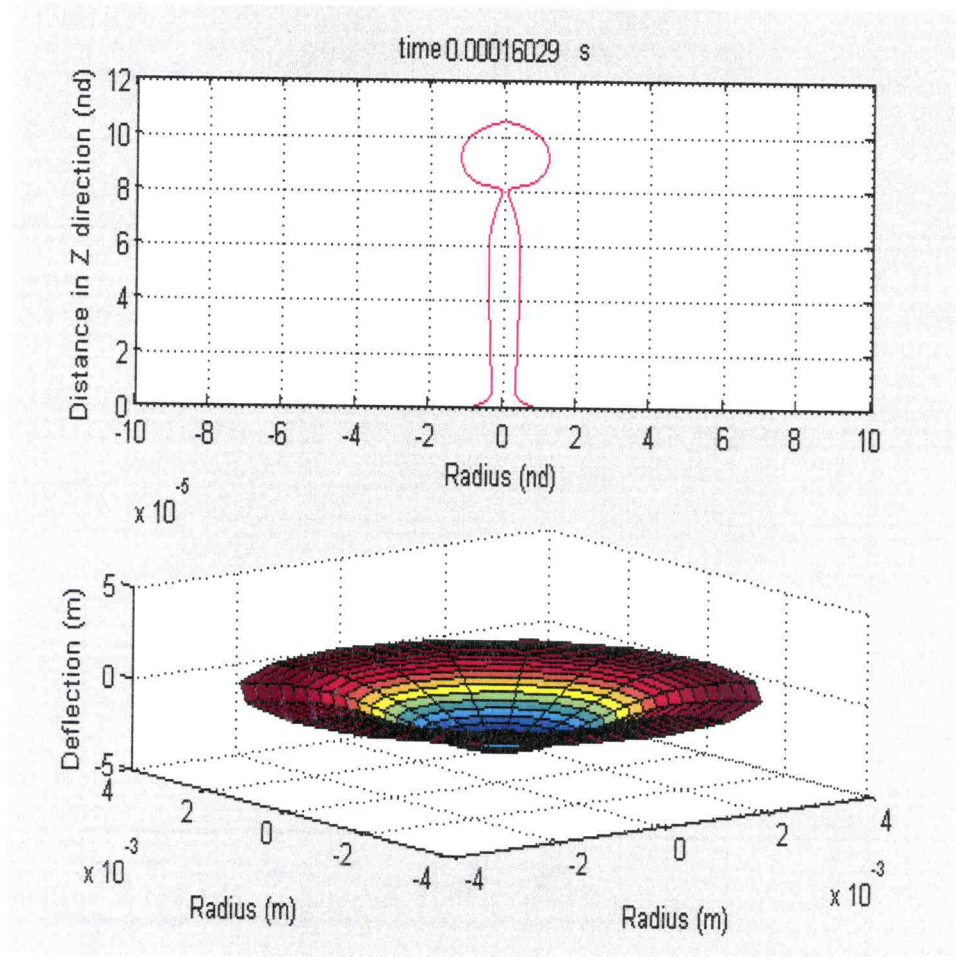


Figure 5.6b Liquid column shape at $t = 0.00016029$ s

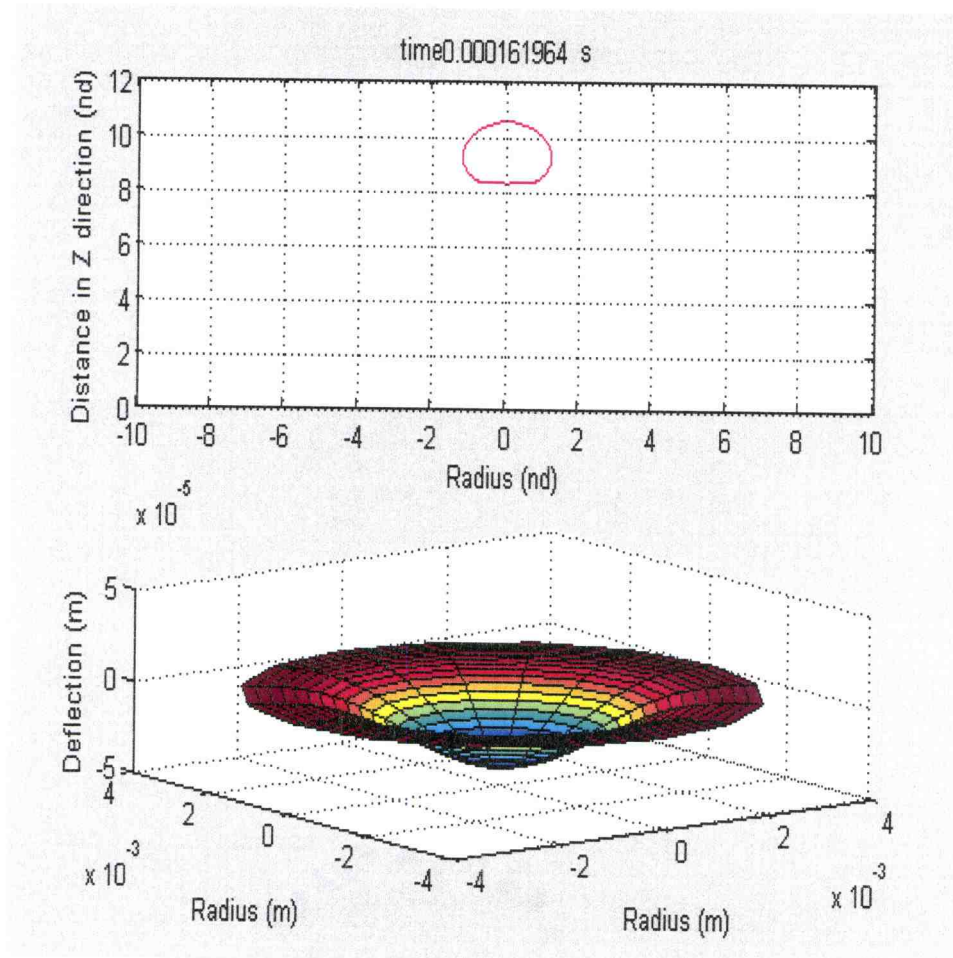


Figure 5.6c Liquid column shape at $t = 0.0001619$ s

The simulation is followed by the process of determining the level of effect at each excitation component plays on the droplet formation. The relationship between Young modulus and droplet formation is presented figures 5.7 through 5.9.

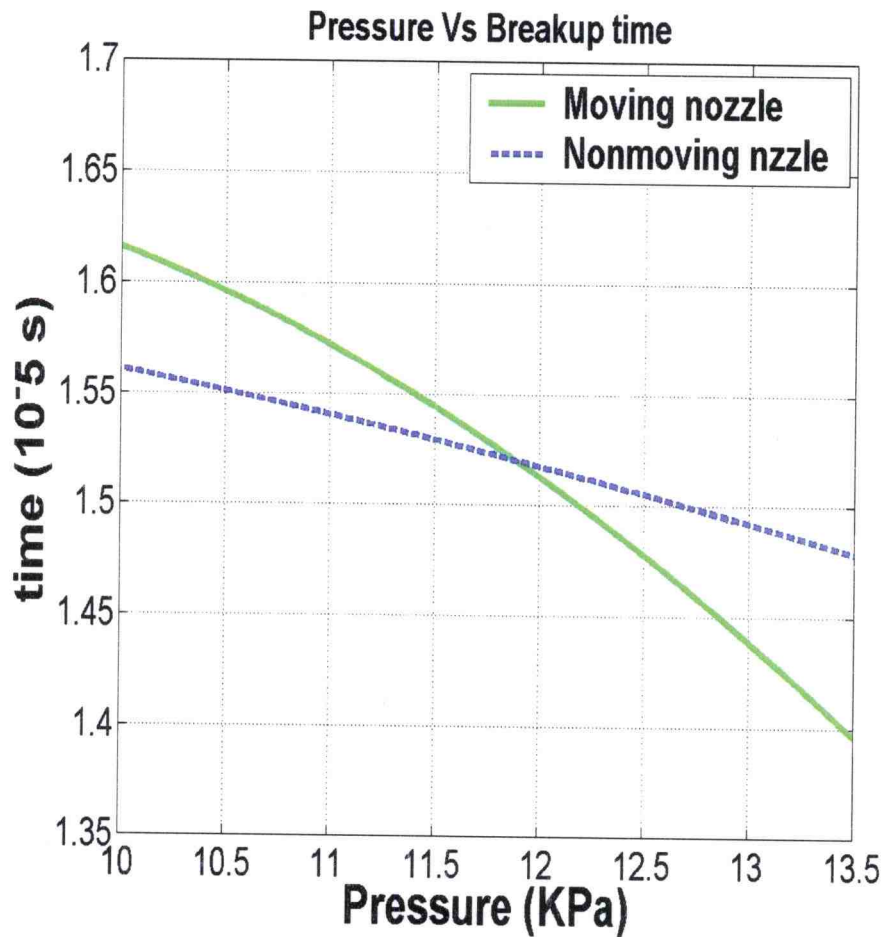


Figure 5.7 Relation between pressure and breakoff time

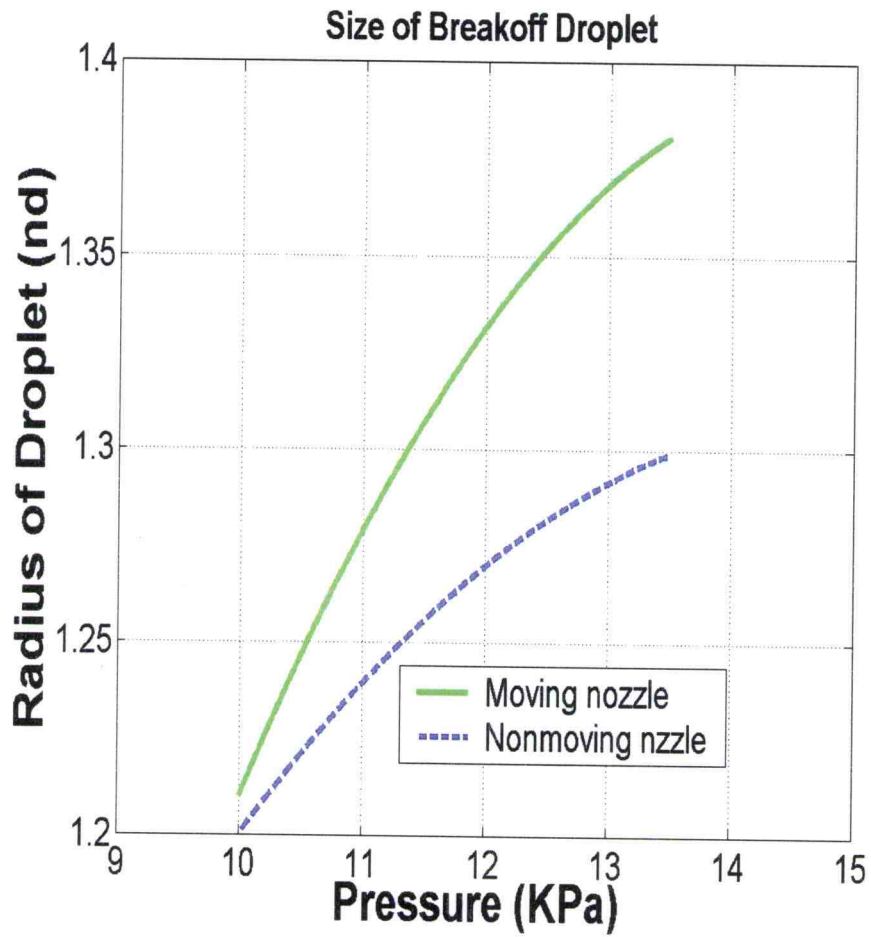


Figure 5.8 Relation between pressure and radius of droplet after breakoff

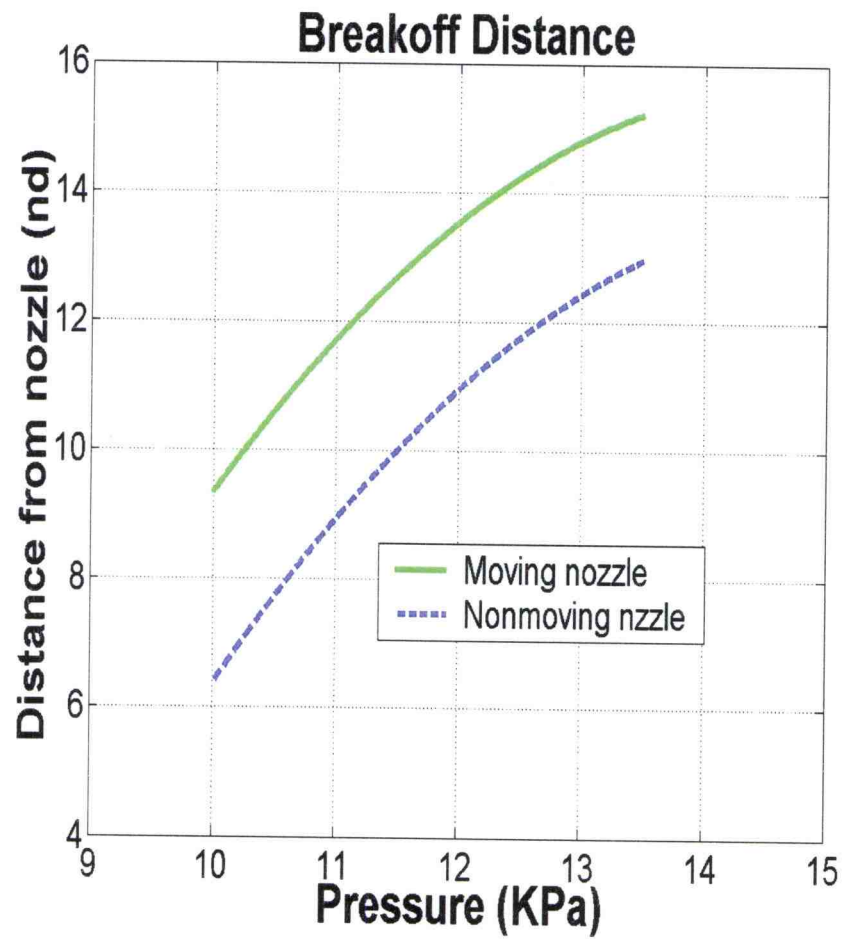


Figure 5.9 Pressure vs distance of droplet after break off

Further investigation, the research then focuses on the plate material, since it is considered as one of the affecting components. Plate's flexibility can cause changes in plate vibration; therefore, it is appropriate to assume that this component has a high potential for being one of the factors which affect the formation of droplet. Figures 5.10 through 5.12 show simulation results for different plate flexibility at each characteristic of droplet breakoff stage.

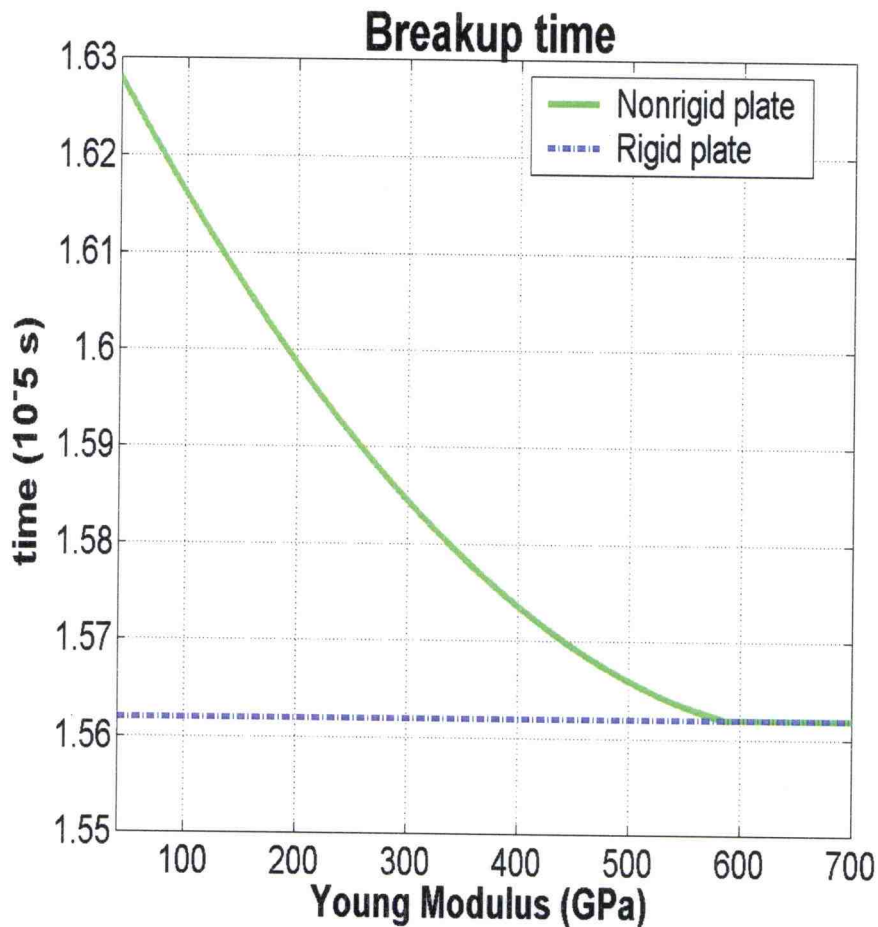


Figure 5.10 Young modulus vs breakup time

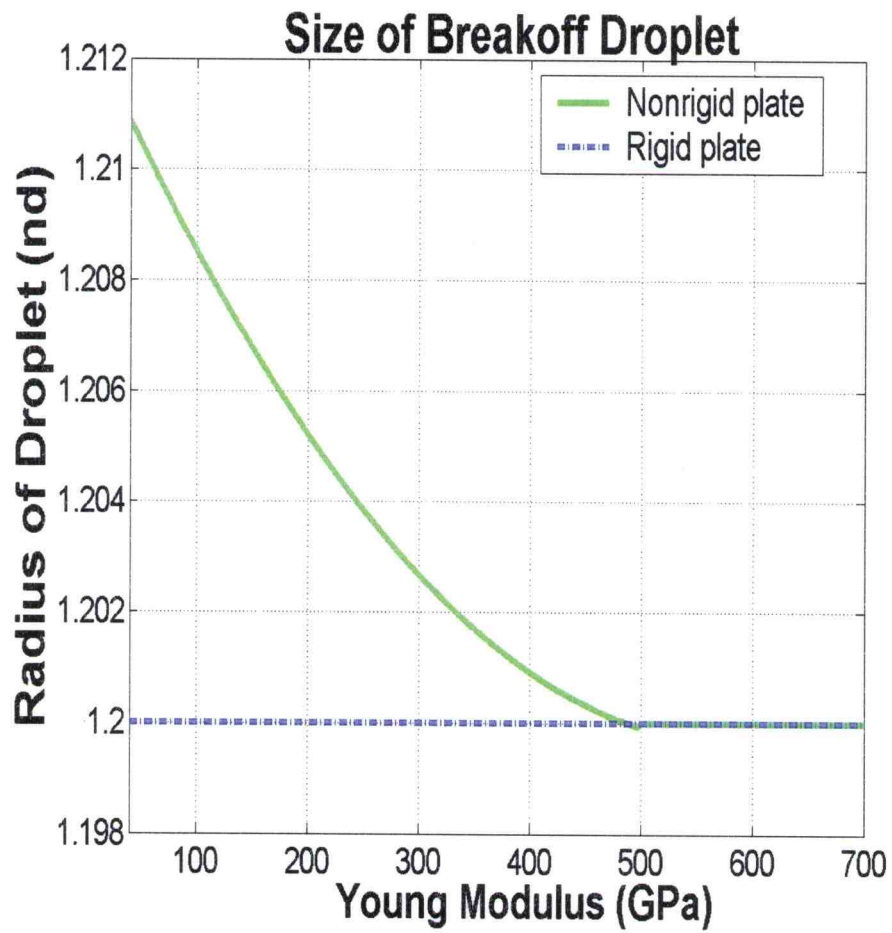


Figure 5.11 Young modulus vs droplet size

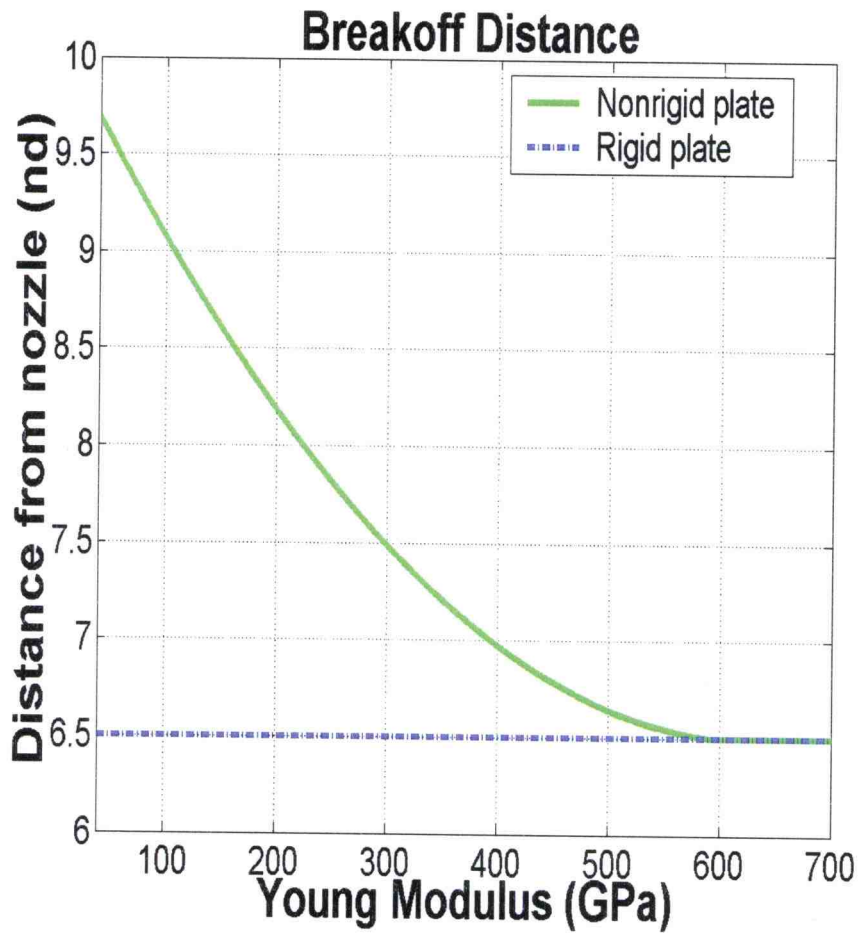


Figure 5.12 Young modulus vs breakoff distance

CHAPTER 6

CONCLUSION

6.1 Conclusion

The original thin plate equation presented in equation 3.25 in this thesis is best considered as an ideal definition of plate vibration. However, the equation is presented with out damping term. After running the simulation of this equation, the result in figure 5.1 shows that the solutions are not compatible to the physical condition of plate vibration. These results lead to the assumption that 1% damping ratio should be applied to the system. The application of 1% damping ratio provides only minimal change in the amplitude response, but the vibration behavior, on the other hand, results in a more physical manner. The experiment can be conducted later to determine the exact value of damping ratio by the application of trial-error method. The solution of thin plate equation can be solved by applying either analytical or numerical method to annular plate. Analytical method provides many limitations, and for this reason it only can be used to solve linear plate equations.

The majority of works on plate models in this thesis emphasizes the large deflection plate equation (3.38). Figure 5.3b show the differences that occur between the small deflection and large deflection plate equations at high force amplitude. High force amplitude is a major factor, which contributes to the differences in the responses of plate vibration; therefore, the large deflection plate equation is employed in the droplet simulation model in order to receive more accurate surface deflection of the nozzle when it is subjected to high force amplitude. To validate the large deflection equation solution, it is used to compare the solution of the Energy method and Galerkin method (figure 5.2).

The droplet simulation of the research had focused on the first droplet formation discharging from the nozzle. *The integration of plate vibration and droplet formation model had been developed.* The trade study of droplet formation can be later proceeded by conducting simulation cases with various excitation characteristics and uses of different plate material. According to conducted simulation, the responses of pulse excitation at different force amplitude are examined (see figures 5.7-5.9). The higher amplitude force excitation provides the faster breakoff time, the longer breakoff distance, and the bigger droplet radius than lower force amplitude. The effects of flexibility condition on the droplet formation are summarized in table 6.1.

Droplet \ Material	High Flexibility	High Rigidity
Breakup time	Shorter period	Longer period
Radius of droplet	Slightly Bigger size	Smaller size
Breakup distance	Longer distance	Shorter distance

Table 6.1 Characteristic of droplet formation with high elasticity and rigidity.

In summary, the nonrigid nozzle plate provides for a longer droplet breakoff time, a slightly bigger droplet size and a longer breakup distance away from the nozzle. According to the summarization above, the assumption can be made that the nonrigid nozzle can result in a more efficient first droplet formation where the droplet flows out faster and longer. However, the decision to which characteristic to be used in the production of inkjet is determined by the manufacturer according to their standard and market demand.

6.2 Recommendations for the Future Research

The research of the plate vibration and droplet formation leads to further related fields of study that includes:

1. ***The continuous droplet formation.*** This thesis had only focused on the formation of the first droplet formation at the nozzle plate; therefore, further study of continuous droplet formation with plate vibration should be conducted to learn more about factors which can be a great contribution to efficiently formation of droplet. These factors include, force amplitude, vibration frequency, plate material and so on
2. ***The realistic model of excitation for plate vibration with the depletable volume of ink inside the chamber.*** The assumption of uniform pressure in the chamber is not fully valid, since the ink level is decreasing as the printer get used and it causes the changes in the distribution of pressure applied on the printed pages. With this fact in mind, the realistic model of excitation for plate vibration with depleting volume of ink inside the chamber should be studied in order to gain more efficient results of printing quality.

BIBLIOGRAPHY

- [1] Amabili, M., and Frosali, G., Vibrazioni di piastre anulari immerse in un liquido, Rapparto 4, Dipartimento di Matematica "V. Volterra", University of Ancona, 1994.
- [2] Amabili, M., Modal properties of annular plates vibrating in water, The First International Conference on Vibration Measurements by Laser Techniques, Advances and Applications, Ancona, Italy, 1994, pp. 421-429.
- [3] Adams, R.L., and Roy, J., A one-dimensional numerical model of a droplet-on-demand ink jet, J. Appl. Mech., vol. 53, 1986, pp.193-197.
- [4] Banks, H.T., Silcox, R.J., and Smith, R.C., Numerical Simulations of a Coupled 3-D Structural Acoustics System, Proceedings of the Second Conference on Recent Advances in Active Control of Sound and Vibration, Blacksburg, VA, 1993, pp. 85-97.
- [5] Bogy, D.B., Drop formation in a circular liquid jet, Annu. Rev. Fluid Mech., vol. 11, 1979.
- [6] Chladni, E. F., Entdeckungen ueber die Theorie des Klanges, 1787
- [7] De Santo, D.F., Added mass and hydrodynamic damping of perforated plates vibrating in water, Journal of Pressure Vessel Technology Vol. 103, 1981, pp. 175-182.
- [8] Edward, B.H., The Numerical Solution of Elliptic Partial Differential Equations by the Method of Lines, Revista Columbiana de Matematicas, vol. XIX, 1985, pp.297-312.
- [9] Galerkin, B.G., Compt rend., vol 190, 1930, p. 1047.
- [10] Kamphoefner, F.J., Ink jet printing, IEEE Trans. Electron Devices, ed. 19, 1972.
- [11] Kirchhoff, G., Ges Abhandl(Leipzig), 1882, p. 259.
- [12] Kubota, Y., and Suzuki, T., Added mass effect on disk vibrating in fluid, Transactions of the Japan Society of Mechanical Engineers, vol. 50, 1984, pp. 243-248.

- [13] Lambeck, K., and Makiboglu, S. M., Seamount loading and stress in the ocean lithosphere, J. Geophys. Res., vol. 85, 1980.
- [14] Leissa, W., Vibrations of Plates, NASA SP-160, 1969.
- [15] Levy, S., Bending of Rectangular Plates with Large Deflection, NACA Technical Notes #853, 1942.
- [16] Navier, Résumé des Leçons sur l' Application de la Mécanique, 3rd ed., Paris, 1864.
- [17] Orszag, S.A., and Patera, A.T., Secondary Instability of Wall-Bounded Shear Flows, Journal of Fluid Mechanics, vol. 128, 1983, pp. 347-385.
- [18] Orszag, S.A., Fourier Series on Spheres, Monthly Weather Review, vol. 102, 1974, pp. 56-75.
- [19] Patera, A.T., and Orszag, S.A., Finite-Amplitude Stability of Axisymmetric Pipe Flow, Journal of Fluid Mechanics, vol. 112, 1981, pp.467-474.
- [20] Rao, J.S., Dynamics of Plates, Marcel Dekkar Inc., 1999.
- [21] Schultz, M.H., Spline Analysis, Prentice-Hall, Englewood Cliffs NJ, 1973.
- [22] Southwell, R.V., On the Free Transverse Vibrations of a Uniform Circular Disc Clamped at its Center and on the Effect of Rotation, Proc. Roy. Soc.(London), vol. 101, 1922, pp. 133-153.
- [23] Srinivasan, A.V., Large Amplitude Free Oscillations of Beams and Plates. AIAA Journal, vol. 3, # 10, pp 1951-1953, October 1965.
- [24] Sweet, R.G., High frequency recording with electrostatically deflected ink jets, Rev. Sci. Instrum., vol. 36, 1965
- [25] Timochenko, S.P., and Goodier, J.N., Theory of Elasticity, 3rd ed., Mc Graw-Hill, 1934.
- [26] Timochenko, S.P., and Woinowsky-Krieger, S., Theory of Plates and Shells, 2nd ed., Mc Graw-Hill, 1959.

- [27] Turcotte, D. L., and G. Schubert, Application of Continuum Physics to Geogical Problem, Geodynamics, John Wiley & Sons, 1982, pp. 104-133.
- [28] Ugural, A.C., Stresses in Plates and Shells, 2nd ed., WCB McGraw-Hill, 1999.
- [29] Vogel, S.M., and Skinner, D.W., Natural Frequencies of Transversely Vibrating Uniform Annular Plates, J. Appl. Mech., vol. 32, December 1965, pp.348-351.
- [30] Von Karman, Festigkeitsprobleme in Maschinenbau, Encl. Der Math. Wiss.,vol. 4, 1910, pp.348-351.
- [31] Wah, T., Vibration of Circular at Large Amplitudes, J. Eng. Mech. Div., Proc. Am., Civil Eng., EM 5, October 1963, pp. 1-15.
- [32] Wessel, P., A Re-examination of the Flexural Deformation beneath the Hawaiian Islands, J. Geophys. Res., vol. 98, 1993.
- [33] Wessel, P., Analytical solutions for 3-D Flexural Deformation of Semi-infinite Elastic Plates, Geophys. J., Vol. 124, 1996.
- [34] Yang, G.Z., Droplet prediction for inkjet cartridge, Master degree thesis, Department of Mechanical Engineering, Oregon State University, Fall 2003.